Information Sciences 698 (2025) 121757

Contents lists available at ScienceDirect

Information Sciences

journal homepage: www.elsevier.com/locate/ins

Integrated information system based on Q-learning algorithm and multi-objective particle swarm optimization with molecular fuzzy-based decision-making for corporate environmental investments

Hasan Dinçer [a,d,*], Serhat Yüksel [a,d], Gabriela Oana Olaru [b], Serkan Eti [c]

[a] School of Business, Istanbul Medipol University, Istanbul, Turkey
[b] School of Communication, Istanbul Medipol University, Istanbul, Turkey
[c] IMU Vocational School, Istanbul Medipol University, Istanbul, Turkey
[d] Research Center for Sustainable Economic Development, Khazar University, Baku, Azerbaijan

A R T I C L E I N F O

Keywords:
Q-learning algorithm
Molecular fuzzy sets
MORAN
Swarm optimization
Environmental performance

A B S T R A C T

Determining the most important criteria is a great necessity to increase the environmental performance of renewable energy projects. This situation helps to reach cost efficiency and effective use of limited resources. However, there are very few studies in the literature where priority analysis is made for these factors. This condition indicates an important gap in the literature on this subject. Accordingly, this study aims to identify the most convenient investment strategies to increase the environmental performance of renewable energy projects. First, the balanced expert dataset is generated via Q-learning algorithm and multi-objective particle swarm optimization. In the following step, selected criteria are weighted with molecular fuzzy cognitive maps approach. The final stage consists of ranking the alternatives with fuzzy molecular ranking (MORAN). The contribution of this study to the literature is to define the most appropriate investment strategies to increase the environmental performance of these projects by generating a new decision-making model. Integrating molecular geometry into decision-making processes increases both the originality and effectiveness of the model. Thus, it is possible to calculate the degrees with a more scientific infrastructure. Integrating Q-learning and swarm optimization techniques into the decision-making model also increases the superiority of the model. In this context, the optimization technique is used to obtain the importance weights of the experts. The findings denote that energy capacity expansion plays the most important role in improving the environmental performance of businesses because it has the greatest weight (0.2563). Return on investment is another factor that plays an important role in increasing this performance with the weight of 0.2559. Geothermal and hydropower are found as the most successful renewable energy types regarding environmental performance improvement since they have the highest aggregated values (0.534 and 0.620). Carbon tax is an important policy application to increase renewable energy capacity. With the help of this tax, fossil fuels lose their competitive advantage significantly. As a result, this situation has a positive contribution to the increase of the renewable energy projects.

* Corresponding author.
E-mail addresses: hdincer@medipol.edu.tr (H. Dinçer), serhatyuksel@medipol.edu.tr (S. Yüksel), gabriela.olaru@medipol.edu.tr (G.O. Olaru), seti@medipol.edu.tr (S. Eti).

https://doi.org/10.1016/j.ins.2024.121757
Received 2 September 2024; Received in revised form 13 December 2024; Accepted 14 December 2024
Available online 16 December 2024

1. Introduction

It is very important to increase the environmental performance of renewable energy investments. Improving the environmental performance of these projects contributes to further reducing carbon emissions. This allows for a more successful fight against the global warming problem. In this way, the negative effects of climate change can be minimized. On the other hand, this situation also plays a very important role in increasing social acceptance. Projects with high environmental performance are more accepted by local communities. This situation positively develops the image of the projects in the eyes of the society. Thus, the products are preferred by more customers. This provides a very serious competitive advantage to renewable energy investors. By increasing environmental performance, these projects can be more successful in legal compliance [1]. In this case, businesses can comply with legal rules more successfully. Similarly, projects with higher environmental performance can more easily receive government support. This situation is very critical for easier access to the required financial resources.

To increase the environmental performance of renewable energy projects, some factors need to be improved. Carbon emission efficiency is quite effective on the environmental performance of renewable energy projects. Efficient systems that reduce carbon emissions also allow for the reduction of energy production costs. In this way, projects can become more profitable. Return on investment is another issue that is effective on the environmental performance of these projects [2]. To provide high returns, projects are generally managed with a focus on cost effectiveness and efficiency. In this way, it is possible to increase the environmental performance of projects. Moreover, energy capacity expansion is necessary to increase the efficiency of this process. With the increase in the rate of renewable energy use, the dependency on fossil fuels decreases. This situation contributes significantly to the improvement of air quality. Similarly, capacity expansion also provides the opportunity to increase energy efficiency [3]. Environmental compliance has a significant effect on the environmental performance of renewable energy projects. Emission standards can be determined depending on environmental compliance. Thanks to these standards, it is much more possible to reduce the carbon footprint of renewable energy projects.

Identifying the most important criteria is a great necessity to increase the environmental performance of renewable energy projects. Determining critical environmental criteria supports projects to use limited resources in the most effective way. This helps businesses to achieve cost efficiency [4]. If these factors are not determined, businesses can implement wrong strategies. This causes investment decisions to lead to very high costs. These increasing costs can also cause financial problems for businesses. In addition to this situation, by determining the most important criteria, the right decisions can be made to minimize the negative effects of projects on the environment. This situation allows financial performance to be increased in a shorter time. If these important factors are not clearly understood, businesses can make wrong investment decisions. This situation negatively affects the financial performance of businesses [5]. Due to these conditions, the most critical variables need to be determined.

Determining appropriate strategies to increase the environmental performance of renewable energy projects is of critical importance for sustainable development goals and combating global warming. However, there are very few studies in the literature where priority analysis is made for these factors. There is no consensus in the literature on which indicators are of the highest importance and which strategy alternatives should be implemented first to improve the environmental performance of renewable energy projects. Therefore, existing studies are insufficient to evaluate the environmental impacts of investment strategies. This situation does not provide a definitive guide as to which strategies should be implemented as a priority to improve environmental performance. In addition to these issues, the decision-making models used cannot fully manage model uncertainties. This situation significantly reduces the reliability of the results obtained. In summary, the lack of sufficient number of studies to determine which indicator is the most important emerges as a very important gap in this literature. In other words, there is a strong need for a new study that makes a priority analysis regarding the performance indicators of the environmental performance of renewable energy projects.

Accordingly, this study aims to identify the most convenient investment strategies to increase the environmental performance of renewable energy projects. To reach this objective, a novel model has been constructed that has three different stages. In the first stage, the balanced expert dataset is generated via q-learning algorithm and multi-objective particle swarm optimization. In this context, velocity, global best position and reward/penalty degrees are calculated. In the next step, with molecular fuzzy cognitive maps approach, selected criteria are weighted. In this process, fuzzy vectors, dot product and cosine of angle are computed. The final stage includes ranking the alternatives with fuzzy MORAN. Within this framework, normalized, angle decision and final decision values are identified. By considering these issues, the research questions of this manuscript are defined as follows.

(1) Which performance indicators for the corporate environmental effectiveness with renewable energy investments have the highest importance weights?

(2) Which renewable energy alternatives should be priorly focused on for the corporate environmental performance improvements?

The motivation for this study stems from the need to determine the most appropriate investment strategies to increase the environmental performance of renewable energy projects. The environmental performance of these projects is of critical importance for minimizing the global warming problem and achieving sustainable development goals. However, there is no consensus in the literature on which indicators are of the highest importance and which strategy alternatives should be implemented first. On the other hand, investments aimed at improving environmental performance are increasing. However, there are no comprehensive enough guidelines on which strategic steps should be implemented as a priority in these projects. In other words, it is not clear which renewable energy alternatives should be prioritized to ensure performance effectiveness. Clarifying this situation allows investors to make the right investment decisions in a shorter time. Decision-making models are a methodology that can be applied to determine the most important variables among many variables affecting a goal [6]. Therefore, this technique can also be taken into consideration in determining the most appropriate investment strategies to increase the environmental performance of renewable energy projects [7]. To increase the effectiveness of this process, the criticisms made regarding the currently developed models should be taken into consideration. In this way, the uncertainty in the process can be reduced more easily and this will increase the reliability of the results to be obtained. Moreover, it is also very significant to select the appropriate techniques while creating a new decision-making model. For instance, the performance indicators for the corporate environmental effectiveness with renewable energy investments can have a strong influence on each other. Because of this condition, selected weighting techniques should considered the causality relationship between these items.

The contribution of this study to the literature is to determine the most appropriate investment strategies to increase the environmental performance of renewable energy projects by creating a new decision-making model. In this context, it is possible to mention both the theoretical and methodological contributions of the study. The most significant contribution of the study in theoretical terms is the calculation of which indicators have the greatest weight to increase the environmental performance of renewable energy projects. This situation has a significant guiding quality for energy investors. One of the most important contributions of determining these factors is the effective use of resources. The limited human and financial resources of businesses can be used effectively by determining these priority strategies. Thus, it is possible to make the right investment decisions without incurring very high costs. On the other hand, the study also has some methodological contributions. The basic advantages of the proposed model are given below.

(1) Integrating molecular geometry into decision-making processes increases both the originality and effectiveness of the model. One of the most criticized issues in decision-making models is the inability to effectively manage uncertainty. This situation negatively affects the success of the results obtained. A number of different shapes are used in molecular geometry. These shapes define how atoms are arranged in a molecule and how they are positioned relative to each other. These shapes are taken into consideration in the degree calculation in the fuzzy decision-making process. Thus, it is possible to calculate both membership, non-membership and hesitancy degrees with a more scientific infrastructure. This allows degree calculations to be performed more accurately. On the other hand, the molecular geometry infrastructure can also be used in the calculation of normalized values. Furthermore, the integration of different molecular geometry shapes into the normalization process enables testing the consistency of the results. In this way, it is possible to reach more effective criterion weights and alternative rankings. Molecular fuzzy sets, which are created by combining molecular geometry and fuzzy logic, offer some important advantages over other types of fuzzy numbers in the literature. Intuitionistic fuzzy numbers use a single membership and rejection degree [8]. Molecular fuzzy sets are not limited to these. In this process, complex situations can be managed much more successfully by using the geometric properties of each molecule [9]. On the other hand, these sets calculate degree values more precisely compared to Pythagorean numbers [10]. Furthermore, normalization calculations with type-2 numbers are quite complicated [11]. Molecular fuzzy sets allow this process to be carried out more effectively.

(2) Integrating Q-learning and swarm optimization techniques into the decision-making model also increases the superiority of the model. In this context, the optimization technique is used to obtain the importance weights of the experts. Thanks to this technique, the weights of the experts are obtained based on the demographic information of the experts. In this framework, an objective approach can be offered in obtaining the expert weights. Similarly, since the Pareto priority solution sets are considered, balanced solutions can be offered in the goal of finding expert weights. Q-learning revises the opinions of other experts according to the best expert. In this framework, the swarm optimization technique is also taken into consideration in selecting the best expert. As a result, it is possible to correctly determine the importance weights of the experts. This contributes to reaching more accurate analysis results. These applications offer a more adaptive, flexible and accuracy-oriented process compared to other methods. Genetic algorithms also use an evolutionary process to find the best expert. To achieve optimization in this process, the population size must be increased [12]. This causes a significant increase in transaction costs. Swarm optimization provides optimization in a more flexible way. This significantly increases the effectiveness of the results obtained. Artificial neural networks approach can also be considered for calculating the importance weights of experts [13]. This technique is used to learn the relationships in large data sets. However, its direct use in determining the importance weights of experts can be complicated. Q-learning requires less data. This method accelerates the decision-making process when combined with swarm optimization. This also supports the increase in the accuracy of the analysis results.

(3) A new ranking technique (MORAN) is introduced in this study. This situation has an increasing impact on the originality of the proposed model. There are lots of criticisms to the existing ranking model. For example, in the calculation steps of VIKOR, only the distance to the positive ideal solution is considered. However, the distance to the negative optimal solution is not computed in this process. This situation is criticized by many different scholars because it negatively affects the performance of the findings. There are also some similar criticisms for other ranking techniques. To overcome these problems effectively, MORAN technique is proposed by integrating molecular geometry into the ranking process. This new technique provides an opportunity to understand the causal directions between the alternatives. The MORAN technique has some advantages over the multi-objective optimization by ratio analysis (MOORA) method. MOORA evaluates the data linearly and processes it with certain coefficients. On the other hand, this structure may be limited in cases of uncertainty. MORAN, on the other hand, uses molecular geometry for uncertainty management [14]. Owing to this issue, more accurate results can be obtained when working with uncertain and incomplete information. Similarly, MOORA evaluates the data with ratio analysis [15]. This situation may be limited especially when working on multi-dimensional data. On the other hand, MORAN can analyze multi-dimensional data with molecular structures in more detail.

The organization of this study is as follows. A new decision-making model is proposed to fill this gap in the literature. The details of the stages of this model are given in Section 2. With this proposed model, criteria weights and alternative rankings can be realized. The details of these issues are shown in Section 3. The results obtained are compared with the findings of similar studies in the literature in Section 4. Moreover, information about the main results, contributions, limitations and future work suggestions is given in Section 5.

2. Proposed research models

Since the main purpose of the study is to evaluate the corporate environmental performance of renewable energy investments, it is necessary to weight the factors affecting the corporate environmental performance of renewable energy investments and to list the alternatives for renewable energy investments within this scope. Since numerical data cannot be obtained in the analysis of these purposes, analysis is carried out with multi-criteria decision-making models. At this stage, molecular fuzzy sets are used to include the uncertainty in linguistic expressions in the analysis.

Fig. 1 depicts the fuzzy hybrid decision-making model, which systematically integrates advanced methodologies, including Multi-Objective Particle Swarm Optimization (MOPSO), Q-learning, Molecular Fuzzy Cognitive Maps (MFCM), and Fuzzy Molecular Ranking (MORAN). This model addresses the prioritization and evaluation of renewable energy alternatives to improve environmental performance, incorporating uncertainty, expert assessments, and multi-dimensional relationships among decision criteria. Below is the detailed explanation of how MOPSO and other operators are combined across the three stages of the model.

The weights derived in Stage 1 serve as inputs for weighting criteria and ranking alternatives, ensuring consistency across all stages. The iterative optimization process enhances reliability by managing the Pareto-optimal solutions dynamically. However, the combination of molecular geometry and fuzzy logic systematically addresses linguistic vagueness and multi-dimensional dependencies.

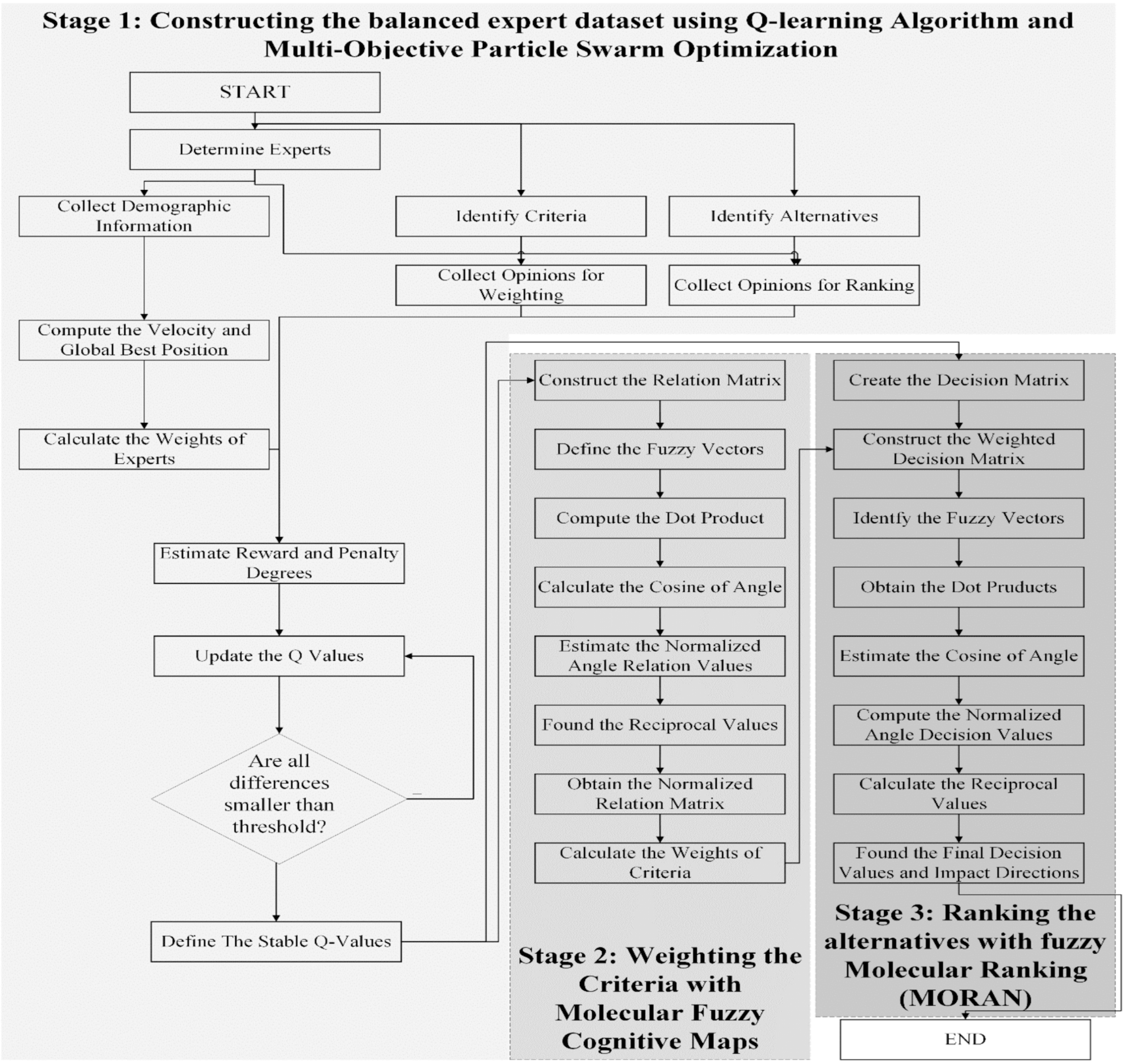

Fig. 1. The details of models.

The operators are interlinked, where outputs from one stage inform the subsequent stage. For instance, the criteria weights influence the MORAN ranking process, while expert weights underpin the entire analysis.

The integration of Q-learning and MOPSO ensures both consistency and adaptability in expert evaluations. The algorithm computes reward and penalty degrees for each expert's evaluations relative to the most experienced expert, as shown in Equations (21) and (22). Q-values are updated iteratively using Equation (23). Convergence is achieved when the changes in Q-values fall below a defined threshold, ensuring a stable and balanced dataset. Expert weights are encoded as particles in a multi-objective decision space. Each particle's velocity and position are updated iteratively using Equations (14) and (16). Pareto-dominance ensures non-dominated solutions are retained, and convergence is evaluated by the stabilization of global best positions. The resulting expert weights are normalized and used in subsequent criteria weighting and alternative ranking stages. The stages of the fuzzy hybrid decision-making model proposed for the evaluation of the corporate environmental performance of renewable energy investments are summarized in Fig. 1.

This study aims to determine effective and priority strategies to increase the environmental performance of renewable energy projects. In this context, both the most important criteria affecting this process and the most suitable renewable energy projects are investigated. In this context, a new and comprehensive decision-making model is established. This model consists of 3 different stages. In the first stage of the model, the importance weights of the experts are calculated according to their demographic structures. In this process, an expert team consisting of three different people is established. The demographic factors of these people are analyzed using the q-learning algorithm and the MOPSO technique. As a result, the importance weights of the experts are calculated. In the second stage of the model, the importance weights of the selected criteria are calculated. To achieve this goal, the molecular fuzzy cognitive maps technique is used. In the last stage of the study, it is determined which of the 5 different renewable energy alternatives is more successful in terms of environmental performance. In this context, the fuzzy molecular ranking technique is taken into consideration. In the ranking process of these alternatives, the criterion weights calculated in the second section are used. On the other hand, in the calculations of criteria weights and alternative rankings performed in the last two stages of the module, the expert weights calculated in the first stage are taken into consideration. In this way, it is possible to achieve more realistic analysis results. The details of the models are presented in this section.

2.1. Molecular fuzzy sets

By integrating the shapes of molecular geometry into the normalization process in fuzzy sets, molecular fuzzy sets are defined. With this contribution to the normalization process of fuzzy sets, more balanced and proportional results are obtained and improved accuracy is provided in the analyses. In addition, the molecular fuzzy set, where the shapes of molecular geometry are integrated to fuzzy sets, allows the consistency of the methodology to be tested with the new approach. The definition and general operations of molecular fuzzy sets set are introduced below [16].

In the discourse universe (X), molecular fuzzy sets (U) are selected for defining relation in multidimensional space. $u_i = (\mu_i, \nu_i, \xi_i)$ is detailed by the condition in Equation (1) with the functions of membership (μ_i), non-membership (ν_i) and hesitancy (ξ_i).

$$\mu_U(u) + \nu_U(u) + \xi_U(u) = 1 \tag{1}$$

The membership degree of molecular fuzzy sets is computed in Equation (2) by normalized angles (θ_u) in molecular geometry.

$$\mu_U(u) = f(\theta_u) = 1 - \frac{\theta_u}{\theta_{max}} \tag{2}$$

where $f(\theta_u)$, is a monotonically function of the normalized angles between 0 and 1, and θ_{max} refers to the maximum normalized angle of the various molecular geometry shape. Degrees (or radians) of various molecular geometry shapes can be calculated. For example, if θ_{max} equals 180° (π radians), a linear shape is obtained, and if this value refers 120° (2/3π), normalized value is computed for Trigonal Planar shape. Similarly, a Tetrahedral shape is found when value of θ_{max} is 109.5° (1.91 rad). For a Trigonal Bipyramidal shape, θ_{max} is equal to 105° (1.83 rad) as average. In another case, θ_{max} equals 90° or π/2 rad and the shape at this angle is an Octahedral shape. However, for molecular fuzzy sets, the degrees of $V_U(u)$ are determined in Equation (3).

$$V_U(u) = \frac{\theta_u}{\theta_{max}} \tag{3}$$

Finally, the degrees of hesitancy for molecular fuzzy sets are estimated with the help of Equation (4).

$$\xi_U(u) = 1 - \left(\left(1 - \frac{\theta_u}{\theta_{max}}\right) + \frac{\theta_u}{\theta_{max}}\right) \tag{4}$$

After the degrees of components of molecular fuzzy sets are obtained, the basic operations computed for A and B fuzzy sets are shared in Equations (5)-(12) where A^- is the complement of A.

$$A \subseteq B \text{if} \mu_A(u) \le \mu_B(u) \text{and} \nu_A(u) \le \nu_B(u) \text{and} \xi_A(u) \ge \xi_B(u), \forall u \in U \tag{5}$$

$$A = B \text{if} A \subseteq B \text{and} B \subseteq A \tag{6}$$

$$A \cup B = \{(u, \max(\mu_A(u), \mu_B(u)), \min(\nu_A(u), \nu_B(u)), \min(\xi_A(u), \xi_B(u)))|u \in U\} \tag{7}$$

$$A \cap B = \{(u, \min(\mu_A(u), \mu_B(u)), \max(\nu_A(u), \nu_B(u)), \max(\xi_A(u), \xi_B(u)))|u \in U\} \tag{8}$$

$$A \cdot B = \{(u, \mu_A(u) \cdot \mu_B(u), \nu_A(u) \cdot \nu_B(u), \xi_A(u) \cdot \xi_B(u))|u \in U\} \tag{9}$$

$$\lambda A = \{(u, \min(\lambda \cdot \mu_A(u), 1), \max(1 - \lambda(1 - \nu_A(u)), 0), \max(1 - \lambda(1 - \xi_A(u)), 0))|u \in U\} \tag{10}$$

$$A^\lambda = \{(u, (\mu_A(u))^\lambda, 1 - \left(1 - \nu_A(u)^\lambda, 1 - \left(1 - \xi_A(u)^\lambda\right)|u \in U\right\} \tag{11}$$

$$A^- = \{(u, \nu_A(u), \xi_A(u), \mu_A(u))|u \in U\} \tag{12}$$

where $\lambda > 0$.

2.2. Multi-Objective particle swarm optimization (MOPSO) for weighting experts

Multi-Objective Particle Swarm Optimization is an improved version of Particle Swarm Optimization (PSO). Thus, a multi-objective problem is solved with the PSO algorithm. The purpose of multi-objective PSO is to produce balanced solutions by creating pareto-optimal alternative results in a multi-objective decision-making problem.

In the literature, there are several widely used multi-objective optimization algorithms to demonstrate its performance in weighting experts for multi-objective decision-making. Non-dominated sorting genetic algorithm II is used for solving complex multi-objective optimization problems [17]. Multi-Objective Differential Evolution is one of other algorithms used in exploring complex decision spaces. It is based on differential evolution for high convergence speed and robust search capabilities in the continuous single-objective domain [18]. However, Strength Pareto Evolutionary Algorithm 2 is introduced for maintaining diversity in solutions and producing distributed pareto front by using a specific clustering mechanism [19].

One of the primary strengths of the MOPSO lies in its convergence speed, particularly due to the unique velocity and position update mechanisms that are specific to the Particle Swarm Optimization framework. MOPSO accelerates convergence by leveraging both cognitive and social components, where each particle is influenced by its own best-known position and the globally best-known position among particles. This dual influence allows particles to quickly converge towards high-quality solutions, especially in the early stages of the search. Another significant advantage of MOPSO is its ability to maintain a balance between exploration (searching new areas of the decision space) and exploitation (refining known solutions). This balance is crucial for obtaining a well-distributed set of solutions on the Pareto front. Also, MOPSO is computationally efficient due to its straightforward mechanics of updating velocity and position without extensive genetic operations. This efficiency is particularly beneficial in high-dimensional or complex objective spaces. Similarly, it is well-suited to dynamic optimization environments, where objectives or constraints may change over time. This adaptability arises from the flexible update process of particles and the algorithm's ability to adjust to new global and personal bests as conditions evolve.

The proposed MOPSO model introduces tailored improvements to adapt to the unique requirements of weighting experts within multi-objective decision-making environments. This methodology includes several key enhancements on the refined particle representation, dynamic velocity adjustment, adaptive position updating, and objective-based expert weighting. For that, we define each particle as a vector in the decision matrix and this presentation effectively captures the multi-dimensional nature of expert weights in the decision-making context. Also, the particle velocity, the central to the exploration–exploitation balance, is updated with the specific inertia weight, cognitive and social coefficients that balance the convergence speed and search capability by controlling volatility degree adjustments per iteration. Accordingly, the initial velocity introduces randomness and adaptiveness, and the particles' positions are updated iteratively based on their velocities. This adaptive approach ensures the optimal convergence toward the pareto-optimal front, yielding more balanced expert weight assignments.

In the MOPSO, each particle represents a potential solution, and its fitness value is a measure of how well this solution meets the multiple objectives of the optimization problem. Each particle's fitness is evaluated based on its ability to meet the objectives defined in the decision-making problem. For this expert-weighting context, we consider criteria such as expertise level, experience, and performance metrics (e.g., precision, consistency). These criteria contribute to the particle's overall fitness, guiding particles towards the most balanced expert weights. The fitness of each particle is not based on a single value but rather on how well it performs relative to other particles across all objectives. We assess particle fitness based on Pareto-dominance, where non-dominated particles (those that perform well across all objectives without being outperformed by others) are considered optimal and added to the Pareto front.

However, particles in this context represent sets of weights for the experts, encoded as vectors in the decision space. These weights are continuous values constrained between 0 and 1 to ensure a realistic weighting scheme. The vector encoding allows each particle to explore different combinations of expert weights in a structured way. Particles are initialized with random weights within the specified bounds (e.g., between 0 and 1) to create diverse starting positions. This randomness helps in exploring various expert weight combinations early in the optimization.

The iterative process of MOPSO involves updating each particle's position and velocity to optimize the weights assigned to experts. Randomly initializing particles with position vectors and velocity vectors for each particle as well as setting initial personal best positions and global best position are presented as the first stage of the specific iterative steps. The calculation of the fitness of each particle and the evaluation of each particle's position against all objectives and identifying non-dominated solutions to form the Pareto front are among the following stages of the iterative steps. Also, the updating personal and global bests as well as each particle's velocity based on cognitive, social, and inertia components are used for the next stages of this iterative steps. At the final stage, the convergence check is applied by evaluating whether the change in global best positions is below a defined threshold indicating convergence. Once convergence is achieved, the final positions of the non-dominated particles represent the Pareto-optimal weights for the experts. These weights are balanced across all objectives, ensuring a robust weighting scheme.

The details of MOPSO are summarized as follows [20].

First, the particle presentation (X_i) is obtained for the potential solution. The X_i defined as a vector in the decision matrix is shown in Equation (13) with the initial position of the particle (x_i).

$$X_i = \{x_{i1}, x_{i2}, \cdots, x_{in}\} \tag{13}$$

where x_{ij} refers the j-th decision position of the i-th particle. The velocity of each particle is computed using the Equation (14). While $V_{ij}(t)$ represents the degree of volatility in the t-th interaction, $V_{ij}(t+1)$ is the updated value of this degree.

$$V_{ij}(t+1) = \omega V_{ij}(t) + c_1 r_1 \left(P_{ij}(t) - X_{ij}(t)\right) + c_2 r_2 \left(P_{gb_j}(t) - X_{ij}(t)\right) \tag{14}$$

The performance of multi-objective algorithms can be highly sensitive to parameter settings, and to ensure a fair comparison, we based our parameter selection on widely accepted values from the literature, along with some fine-tuning based on preliminary experiments in our specific context. ω is the inertial weight, which is equal to 0.5 and defines the exploration capacity. This value is chosen based on common practice in the literature and further validated in our initial tests to maintain particle stability and efficient convergence. P_{ij} means the best position of each particle. While c_1 is defined as the cognitive coefficient, the value of c_2 is considered as the social coefficient. The value of these two coefficients in the analysis is equal to 1.5. It encourages a balance between individual and group influence in particle movement. These settings are well-aligned with literature recommendations [21] and enhance the algorithm's ability to refine expert weights. The r_1 and r_2 are random values between 0 and 1.

The global best position among the decision alternatives is symbolized as P_{gb_j}. The initial velocity $\left(V_{ij}(1)\right)$ is estimated using Equation (15) with values of the maximum $\left(P_{max_j}\right)$ and minimum $\left(P_{min_j}\right)$ of i-th item.

$$V_{ij}(1) = \partial \times \left(P_{max_i} - P_{min_i}\right) \times r \tag{15}$$

where ∂ equals to 0.1 and $-1 \le r \le 1$. Afterwards, the position of each particle is updated with the help of Equation (16).

$$X_{ij}(t+1) = X_{ij}(t) + V_{ij}(t+1) \tag{16}$$

The personal and global best positions of the particles are iteratively calculated by Equations (17)-(19).

$$P_{ij}(t+1) = Best\left(P_{ij}(t), X_{ij}(t+1)\right) \tag{17}$$

$$P_{gb_j}(t+1) = Best\left(P_{gb_j}(t), \{X_{ij}(t+1)\} alli\right) \tag{18}$$

$$\left|P_{gb_j}(t+1) - P_{gb_j}(t)\right| < \epsilon \tag{19}$$

This iterative process is repeated until the differences in the global positions remain less than 0.001 (ϵ). After the iteration condition is tested, Equation (20) is used for computing the average values of criteria.

$$\frac{1}{n}\sum_{i=1}^{n} P_{ij} \tag{20}$$

In results of Equation (20), the weights of experts are obtained.

2.3. Q-learning algorithm for Unbalanced Expert evaluations

The experience of experts is one of the most important components for expert opinion-based problem-solving strategies. The evaluation provided by highly qualified specialists carries greater weight. Because of this, the Q-learning algorithm is proposed, in which the learning rate employs penalty and reward factors based on the judgment of the most experienced expert to determine the opinions of other experts. The Q-learning algorithm's steps are listed below [22].

In Q-learning algorithm, reward and penalty degrees are computed among the best expert and other experts. Equation (21) and (22) are about the calculation of the reward degree $\left(R_{s,a}\right)$ and penalty degree $\left(P_{s,a}\right)$ for each state-action pair (s, a).

$$R_{s,a} = r \cdot \left(Q_{s,a(bestDM)} - Q_{s,a(otherDM)}\right) \tag{21}$$

$$P_{s,a} = p \cdot \left(Q_{s,a(otherDM)} - Q_{s,a(bestDM)}\right) \tag{22}$$

While $Q_{s,a(bestDM)}$ in Equation (21) refers the evaluation of the best expert, Q-values are determined as the initial value. Likewise, $Q_{s,a(otherDM)}$ means the assessment of the other experts. While the r equals reward factor, p is penalty factor. The r is used for setting the quantify and the positive feedback. The p is used or quantifying the negative feedback among the experts. Afterwards, the Q values are updated using Equation (23).

$$Q'_{s,a} = Q_{s,a(bestDM)} + \alpha \cdot (R_{s,a} - P_{s,a}) \tag{23}$$

where, the updated Q values is symbolized as $Q'_{s,a}$ and α is learning rate and used for ensuring efficient and stable learning process from new experiences. The low value of α is that learning process is slowly but more stability. However, in case of the high value of α, the analysis is more responsive and rapid with the risk of overshooting. The optimal Q values are estimated with maximum value of difference of $Q'_{s,a}$ and initial Q values with the help of Equations (24) and (25).

$$\Delta_{s,a} = |Q'_{s,a} - Q_{s,a}| \tag{24}$$

$$\Delta_{max} = \max_{s,a}\{\Delta_{s,a}\} \tag{25}$$

The iteration process continuous until $\Delta_{max} < \varepsilon$. If this convergence check is achieved for threshold values (ε), the values become stationary for the final Q values.

2.4. Molecular fuzzy cognitive maps

To analyze decision support systems with interacting components for nonlinear situations, fuzzy cognition maps are employed. Thus, the weights of the criteria are also determined while the relationship between the factors is described. The steps for integrating cognitive maps with molecular fuzzy numbers are outlined below and are used in this article [23].

Molecular cognitive maps start with experts identifying the dependency degree of inter-criteria. A relation matrix is constructed from linguistic opinions of experts. Then, the molecular fuzzy relation matrix (ς_k) is created in Equation (26) with the fuzzy number equivalents of the experts' linguistic opinions. Elements $\left(\varsigma_{ij} = \left(\varsigma_{\mu_{ij}}, \varsigma_{\nu_{ij}}, \varsigma_{\xi_{ij}}\right)\right)$ of this matrix refers the influence degree of criterion i stated in the row over the criterion j given in the column.

$$\varsigma_k = \begin{bmatrix} 0 & \varsigma_{12} & \cdots & \cdots & \varsigma_{1n} \\ \varsigma_{21} & 0 & \cdots & \cdots & \varsigma_{2n} \\ \vdots & \vdots & \ddots & \cdots & \cdots \\ \vdots & \vdots & \vdots & \ddots & \vdots \\ \varsigma_{n1} & \varsigma_{n2} & \cdots & \cdots & 0 \end{bmatrix} \tag{26}$$

where, the number of experts is k. With the help of Equation (27), the aggregated values of the molecular fuzzy direct relation matrix (ς) are estimated.

$$\varsigma = \left(\bigcup_{i=1}^{k}\varsigma_i\right) = \left\{\left(u, \frac{1}{k}\sum_{i=1}^{k}\mu_{\varsigma_i}(u), \frac{1}{k}\sum_{i=1}^{k}\nu_{\varsigma_i}(u), \frac{1}{k}\sum_{i=1}^{k}\xi_{\varsigma_i}(u)\right)|u \in U\right\} \tag{27}$$

Afterwards, the fuzzy vectors of the relation matrix with n rows and n columns are constructed by molecular fuzzy number components. The fuzzy vectors (u_i) shown in Equation (28) are determined for each criterion relation except for the self-connections.

$$u_i = \left[(\mu_{i1}, \nu_{i1}, \xi_{i1}), (\mu_{i2}, \nu_{i2}, \xi_{i2}), \cdots \left(\mu_{i(n-1)}, \nu_{i(n-1)}, \xi_{i(n-1)}\right)\right] \tag{28}$$

With these fuzzy vector pairs, the dot product $(u_i.u_j)$ is computed using Equation (29).

$$(u_i.u_j) = \sum_{t=1}^{n-1}\left(\mu_{i,t}\cdot\mu_{j,t} + \nu_{i,t}\cdot\nu_{j,t} + \xi_{i,t}\cdot\xi_{j,t}\right) \tag{29}$$

For each fuzzy relation vector pair, the cosine of the angle $\left(\cos(\theta_{u_i,u_j})\right)$ is obtained by Equation (30) using the cosine similarity and the magnitude of the u_i.

$$\cos(\theta_{u_i,u_j}) = \frac{(u_i.u_j)}{\left(\sum_{t=1}^{n-1}\left(\mu_{i,t}^2 + \nu_{i,t}^2 + \xi_{i,t}^2\right)\right).\left(\sum_{t=1}^{n-1}\left(\mu_{j,t}^2 + \nu_{j,t}^2 + \xi_{j,t}^2\right)\right)} \tag{30}$$

The angle value $\left(\theta_{u_i,u_j}\right)$ is calculated by the inverse cosine function (cos^{-1}) shown in Equation (31) and the value of function is between in 0 and π (0 and 180^0).

$$\theta_{u_i,u_j} = cos^{-1}\left(\cos(\theta_{u_i,u_j})\right) \tag{31}$$

The normalization of angle values $\left(norm\left(\theta_{u_i,u_j}\right)\right)$ with the maximum value of the angle relation matrix (θ_{max}) is computed with the help of Equation (32) and the various normalization operations with various molecular geometry shapes are summarized in Equations (33)-(37).

$$norm\left(\theta_{u_i,u_j}\right)_{general} = \frac{\theta_{u_i,u_j}}{\theta_{max}} \tag{32}$$

$$norm\left(\theta_{u_i,u_j}\right)_{linear} = \frac{\theta_{u_i,u_j}}{\pi} \tag{33}$$

$$norm\left(\theta_{u_i,u_j}\right)_{trigonal_{planar}} = \frac{\theta_{u_i,u_j}}{\frac{2\pi}{3}} \tag{34}$$

$$norm\left(\theta_{u_i,u_j}\right)_{tetrahedral} = \frac{\theta_{u_i,u_j}}{\frac{\pi}{2}} \tag{35}$$

$$norm\left(\theta_{u_i,u_j}\right)_{trigonal_{bipyramidal}} = \frac{\theta_{u_i,u_j}}{\frac{2\pi}{5}} \tag{36}$$

$$norm\left(\theta_{u_i,u_j}\right)_{octahedral} = \frac{\theta_{u_i,u_j}}{\frac{\pi}{3}} \tag{37}$$

The reciprocal values of the normalized angles $\left(recip\left(\theta_{u_i,u_j}\right)\right)$ are estimated using Equation (38).

$$recip\left(\theta_{u_i,u_j}\right) = \frac{1}{norm\left(\theta_{u_i,u_j}\right)} \tag{38}$$

With the help of Equation (39), the normalization of the relationship matrix (NR) presented by Equation (40) is created.

$$N_{ij} = \frac{recip\left(\theta_{u_i,u_j}\right)}{\sum_{j=1}^{n} recip\left(\theta_{u_i,u_j}\right)} \tag{39}$$

$$NR = \begin{bmatrix} 0 & N_{12} & \cdots & \cdots & N_{1n} \\ N_{21} & 0 & \cdots & \cdots & N_{2n} \\ \vdots & \vdots & \ddots & \cdots & \cdots \\ \vdots & \vdots & \vdots & \ddots & \vdots \\ N_{n1} & N_{n2} & \cdots & \cdots & 0 \end{bmatrix} \tag{40}$$

The state vector values given in Equation (41) are constructed.

$$A(t) = [a_1(t), a_2(t), \cdots, a_n(t)] \tag{41}$$

where, the number of iterations is presented with t. In this case, $a_n(t)$ means nth dimension vector, and $A(t)$ refers to the activation levels of the criteria at the t^{th} iteration. $A(0)$ is the initial state vector, each value of which is 1. The initial state vectors are updated using Equations (42) and (43) until $fA(s+1) = fA(s)$.

$$A(t+1) = f(A(t) \cdot NR) \tag{42}$$

$$f(x) = \frac{1}{1+e^{-x}} \tag{43}$$

The sigmoid function is used for normalizing the values. Finally, the weights of criteria (W_j) are found by Equation (44).

$$W_j = \frac{fA(s)_j}{\sum_{j=1}^{n} fA(s)_j} \tag{44}$$

where, the value of $fA(s)$ gives the stabilized state vector for sth iteration.

2.5. Fuzzy molecular ranking (MORAN)

The most newly ranking model in the literature on multi-criteria decision making that takes the relationship between options into account is fuzzy molecular ranking. This method's ability to provide spatial interactions (or relations) between alternatives is by far its greatest advantage. As a result, the study yields more precise results and a thorough ranking. A detailed explanation of the fuzzy MORAN is provided below [24].

At the beginning, linguistic opinions from experts are collected. After that, the decision matrix is constructed. Afterwards, the molecular fuzzy decision matrix (X_k) is identified in Equation (45) with the fuzzy number equivalents of the linguistic opinions of experts. The elements of this matrix $\left(X_{ij} = \left(X_{\mu_{ij}}, X_{\nu_{ij}}, X_{\xi_{ij}}\right)\right)$ give about the information on the alternative i with respect to criterion j stated.

$$X_k = \begin{bmatrix} X_{11} & X_{12} & \cdots & \cdots & X_{1m} \\ X_{21} & X_{22} & \cdots & \cdots & X_{2m} \\ \vdots & \vdots & \ddots & \cdots & \cdots \\ \vdots & \vdots & \vdots & \ddots & \vdots \\ X_{n1} & X_{n2} & \cdots & \cdots & X_{nm} \end{bmatrix} \tag{45}$$

Using Equation (27), the aggregated values of the molecular fuzzy decision matrix (X) are calculated. Later, the weighted decision matrix (B) is created with the help of Equation (46) using weight of criteria (w).

$$B_{ij} = \left(w_j.\mu_{ij}, w_j.\nu_{ij}, w_j.\xi_{ij}\right) \tag{46}$$

The fuzzy vectors of the decision matrix with n rows and m columns are constructed by molecular fuzzy number components. The fuzzy vectors (y_i) given in Equation (47) are created for each relation of alternatives.

$$y_i = [(\mu_{i1}, \nu_{i1}, \xi_{i1}), (\mu_{i2}, \nu_{i2}, \xi_{i2}), \cdots(\mu_{im}, \nu_{im}, \xi_{im})] \tag{47}$$

The dot product $\left(y_i.y_j\right)$ is estimated for fuzzy vector pairs with Equation (48).

$$\left(y_i.y_j\right) = \sum_{t=1}^{n} \left(\mu_{i,t} \cdot \mu_{j,t} + \nu_{i,t} \cdot \nu_{j,t} + \xi_{i,t} \cdot \xi_{j,t}\right) \tag{48}$$

Afterwards, the cosine of the angle $\left(\cos(\theta_{y_i y_j})\right)$ is calculated with the help of Equation (49) according to the cosine similarity and the magnitude of the y_i.

$$\cos(\theta_{y_i y_j}) = \frac{\left(y_i.y_j\right)}{\left(\sum_{t=1}^{m}\left(\mu_{i,t}^2 + \nu_{i,t}^2 + \xi_{i,t}^2\right)\right).\left(\sum_{t=1}^{m}\left(\mu_{j,t}^2 + \nu_{j,t}^2 + \xi_{j,t}^2\right)\right)} \tag{49}$$

The angle values $\left(\theta_{y_i y_j}\right)$ are calculated by the inverse cosine function (cos^{-1}) shown in Equation (50).

$$\theta_{y_i y_j} = cos^{-1}\left(\cos(\theta_{y_i y_j})\right) \tag{50}$$

The general normalization of angle value $\left(norm\left(\theta_{y_i y_j}\right)\right)$ with the maximum value of the angle relation matrix (θ_{y_max}) is computed with the help of Equation (51) and the other normalization process using various molecular geometry shapes are calculated using Equation (52)-(56).

$$norm\left(\theta_{y_i y_j}\right)_{general} = \frac{\theta_{y_i y_j}}{\theta_{y\_max}} \tag{51}$$

$$norm\left(\theta_{y_i y_j}\right)_{linear} = \frac{\theta_{y_i y_j}}{\pi} \tag{52}$$

$$norm\left(\theta_{y_i y_j}\right)_{trigonal_{planar}} = \frac{\theta_{y_i y_j}}{\frac{2\pi}{3}} \tag{53}$$

$$norm\left(\theta_{y_i y_j}\right)_{tetrahedral} = \frac{\theta_{y_i y_j}}{\frac{\pi}{2}} \tag{54}$$

$$norm\left(\theta_{y_i y_j}\right)_{trigonal_{bipyramidal}} = \frac{\theta_{y_i y_j}}{\frac{2\pi}{5}} \tag{55}$$

$$norm\left(\theta_{y_i y_j}\right)_{octahedral} = \frac{\theta_{y_i y_j}}{\frac{\pi}{3}} \tag{56}$$

In the next step, the reciprocal values of the normalized angles $\left(recip\left(\theta_{y_i y_j}\right)\right)$ are computed by Equation (57).

$$recip\left(\theta_{y_i y_j}\right) = \frac{1}{norm\left(\theta_{y_i y_j}\right)} \tag{57}$$

The final decision matrix (F) is created using Equation (58) with the value of final decision matrix $\left(f_{ij}\right)$.

$$f_{ij} = \frac{recip\left(\theta_{y_i y_j}\right)}{\sum_{j=1}^{n} recip\left(\theta_{y_i y_j}\right)} \tag{58}$$

Finally, the aggregated values of F are computed using Equation (59) to estimating of the final ranking.

$$Agg(f_i) = \sum_{j \neq i} f_{ij} \tag{59}$$

The alternatives are ranked according to the values of $Agg(f_i)$ in descending order. The impact of the alternatives is mapped with threshold values. The value is equal the average of the elements of F.

3. Analysis results

The results of the analysis using molecular fuzzy sets identified with the help of Equations (1)-(12) are summarized under this section.

3.1. Constructing The balanced Expert dataset using Q-learning algorithm and Multi-Objective particle swarm optimization

The linguistic opinions from the experts for the relation and decision matrices are collected. For this, the linguistic scales in Table 1 are used.

For the corporate environmental performance with renewable energy investments, the criteria set is constructed from literature reviews. The four criteria are carbon emission efficiency (CAEMEFF), return on investment (RETINV), energy capacity expansion (ENGCAPEX), environmental compliance and standards (ENVCOMSTD). Expert evaluations of the selected criteria are reported in Table 2.

Renewable energy types such as solar, wind, geothermal, biomass and hydropower are also evaluated by experts according to the selected criteria. The opinions about renewable energy types are in Table 3.

For the Q-learning algorithm, the best expert needs to be determined. Therefore, expert weights are calculated with the MOPSO method. For the MOPSO algorithm, demographic information of the experts is analyzed. For this, the initial position of the velocity of the particles based on the demographic information is determined. The results are shared in Table 4.

Experts with doctoral degrees are included in the article. The profession variable is defined according to seniority and numerical coding of this variable is given in the Table 4. Afterwards, the velocity, the updated personal and global best positions are iteratively computed with the help of Equations (13)-(19). The results of these equations are summarized in Table 5.

As can be seen from Table 5, at the end of the fourth iteration, the changes of the global best positions are smaller than the threshold of 0.001. In other words, the results of the fourth iteration are the final results of the MOPSO. The average values of the criteria are computed for weighting the experts using Equation (20). According to the result of Equation (20), experts have the weights as 0.349, 0.321, and 0.330 respectively. According to the weight values, while Expert 1 has the highest weight, Expert 2 has the weakest weight in the expert team.

After determining the best expert, the Q-learning algorithm is applied. Initially, the best expert is considered as Expert 1. Because in the result of the MOPSO method, the highest weight belongs to this expert. Opinions are transformed into fuzzy numbers according to Table 1. The opinions of Expert 1 are accepted as the initial Q value. The opinions of other experts are compared according to the initial Q value. The weights of other experts are the reward factors among experts. Next, the $R_{s,a}$ and $P_{s,a}$ among the experts for the relation and decision matrices are computed using Equations (21) and (22). The reward degree of fuzzy relation matrix is displayed in Table 6.

The reward degree of fuzzy decision matrix is illustrated in Table 7.

Likewise, the penalty degrees among the experts for the relation and decision matrices are calculated. The penalty degree of fuzzy relation matrix is share in Table 8.

Similarly, the penalty degree of fuzzy decision matrix is tabulated in Table 9.

In the next step of analysis, the updated values of the relation and decision matrices are constructed using Equation (23). In this step, learning rate equals 0.1. The updated values of fuzzy relation matrix are shown in Table 10.

Similarly, the updated values of fuzzy decision matrix are given in Table 11.

Table 1
Linguistic Scales.

Linguistic Scales	Fuzzy Numbers (μ_i, ν_i, ξ_i)
Negligible-N	(0.20,.70,.10)
Low-L	(0.40,.50,.10)
Moderate-M	(0.60,.30,.10)
Significant-S	(0.80,.15,.05)
High-H	(0.95,.05,.00)

Table 2
Linguistic Evaluations of The Criteria Relations by The Experts.

Expert 1	CAEMEFF	RETINV	ENGCAPEX	ENVCOMSTD
CAEMEFF		H	H	S
RETINV	S		H	H
ENGCAPEX	S	S		H
ENVCOMSTD	M	M	H	
Expert 2	**CAEMEFF**	**RETINV**	**ENGCAPEX**	**ENVCOMSTD**
CAEMEFF		S	S	S
RETINV	M		H	H
ENGCAPEX	M	M		S
ENVCOMSTD	M	M	H	
Expert 3	**CAEMEFF**	**RETINV**	**ENGCAPEX**	**ENVCOMSTD**
CAEMEFF		H	H	S
RETINV	H		H	H
ENGCAPEX	S	S		H
ENVCOMSTD	S	H	H	

Table 3
Linguistic Opinions of The Renewable Energy Types Relations by The Experts.

Expert 1	CAEMEFF	RETINV	ENGCAPEX	ENVCOMSTD
SOLAR	S	H	S	S
WIND	S	S	H	S
GEOTHERMAL	H	H	H	S
BIOMASS	H	H	S	H
HYDROPOWER	H	H	H	S
Expert 2	**CAEMEFF**	**RETINV**	**ENGCAPEX**	**ENVCOMSTD**
SOLAR	S	M	S	S
WIND	S	S	H	M
GEOTHERMAL	M	H	H	S
BIOMASS	H	H	S	H
HYDROPOWER	H	H	H	M
Expert 3	**CAEMEFF**	**RETINV**	**ENGCAPEX**	**ENVCOMSTD**
SOLAR	S	S	S	S
WIND	S	S	H	S
GEOTHERMAL	H	H	H	S
BIOMASS	S	S	S	S
HYDROPOWER	S	S	H	S

The absolute differences between the Q values of the experts for the relation and decision matrices are calculated using the Equations (24) and (25). This process is iterative and continues until the $\Delta_{max} < 0.02$. At the end of first iteration, the result of absolute difference of fuzzy relation matrix is obtained and shared in Table 12.

Since some values in Table 12 are above the specified threshold value, the iteration steps are repeated. Table 13 is about the absolute difference of fuzzy decision matrix for first iteration.

As in Table 12, some values in Table 13 are greater than 0.02. Therefore, the iteration process is applied for the relation and decision matrices. The stability of Q values with the convergence check for the relation matrix is determined. The matrix is displayed in Table 14.

By the fourth iteration, all absolute differences of fuzzy number degrees for the relation matrix among Expert 1 and Expert 3 remain below the desired value. However, all values among Expert 1 and Expert 2 are less than 0.02 in the first iteration. Iterative absolute differences of fuzzy decision matrix among Expert 1 and Expert 2 are illustrated in Table 15.

As can be seen, the absolute values have become stable in the fourth iteration for Expert 1 and Expert 2, and in the first iteration for Expert 1 and Expert 3. Like this, the stable fuzzy Q values of experts for the relation matrix are seen in Table 16.

Finally, the stable fuzzy Q values of experts for the decision matrix are reported in Table 17.

Thus, Table 16 and Table 17 constructed as a result of the Q-learning algorithm are used for weighting and ranking analyses.

Table 4
Initial Position of The Particles Based on Demographic Information of Experts.

	Age (D1)	Experience in total-year (D2)	Education (D3)	Profession (D4)	Published papers (D5)	Global Experience-year (D6)	Number of licenses and certifications (D7)	Teaching experience-part-time or full-time (D8)	Number of conference participation (D9)	Number of patents (D10)
E1	48	22	1 (PhD)	0.9 (Professor)	52	8	2	22	61	1
E2	50	23	1 (PhD)	0.8(Project Manager)	14	4	5	5	23	8
E3	56	28	1 (PhD)	1 (Chairman of the Board)	21	10	7	2	27	5

Table 5
Velocity, Updated Personal and Global Best Positions for Several Iterations.

	E1 $((V_1)(1))$	E2 $((V_2)(1))$	E3 $((V_3)(1))$	E1 $((P_1)(1))$	E2 $((P_2)(1))$	E3 $((P_3)(1))$	$((P_{gb})(1))$	$((P_{gb})(t)) - ((P_{gb})(t-1))$
D1	−0.54	0.29	−0.77	56.11	56.43	56.00	56	–
D2	0.02	0.14	−0.52	28.29	28.30	28.00	28	–
D3	0.00	0.00	0.00	1.00	1.00	1.00	1	–
D4	0.00	0.00	−0.01	1.01	1.01	1.00	1	–
D5	−3.28	3.36	−1.79	52.00	55.46	52.56	52	–
D6	−0.22	−0.43	0.55	9.98	10.07	10.28	10	–
D7	−0.48	0.01	−0.44	7.00	7.10	7.00	7	–
D8	−1.80	−1.35	1.57	22.00	22.12	23.72	22	–
D9	−2.52	3.57	0.60	61.00	64.57	62.90	61	–
D10	−0.47	−0.36	0.16	8.09	8.00	8.22	8	–
	E1 $((V_1)(2))$	E2 $((V_2)(2))$	E3 $((V_3)(2))$	E1 $((P_1)(2))$	E2 $((P_2)(2))$	E3 $((P_3)(2))$	$((P_{gb})(1))$	$((P_{gb})(t)) - ((P_{gb})(t-1))$
D1	−0.02	0.58	−0.04	54.10	54.81	56.00	56.00	0.00
D2	−0.06	−0.16	0.09	26.45	26.79	28.09	28.00	0.00
D3	0.00	0.00	0.00	1.00	1.00	1.00	1.00	0.00
D4	0.01	−0.01	0.00	0.98	0.96	1.00	1.00	0.00
D5	−0.30	−0.72	−2.42	52.00	43.51	45.54	52.00	0.00
D6	0.71	−0.16	−0.23	9.92	8.74	10.28	10.28	0.28
D7	−0.14	−0.28	0.11	5.85	6.71	7.11	7.00	0.00
D8	−0.05	0.25	1.77	22.26	17.99	17.93	22.26	0.26
D9	−0.27	−1.81	2.08	61.95	52.64	53.90	61.95	0.95
D10	−0.18	−0.27	0.04	6.37	8.16	7.29	8.16	0.16
	E1 $((V_1)(3))$	E2 $((V_2)(3))$	E3 $((V_3)(3))$	E1 $((P_1)(3))$	E2 $((P_2)(3))$	E3 $((P_3)(3))$	$((P_{gb})(3))$	$((P_{gb})(t)) - ((P_{gb})(t-1))$
D1	−3.17	−2.43	−0.02	54.10	54.81	56.00	56.00	0.00
D2	−2.14	−1.94	−0.02	26.45	26.79	28.09	28.09	0.09
D3	0.00	0.00	0.00	1.00	1.00	1.00	1.00	0.00
D4	−0.03	−0.08	0.00	0.98	0.96	1.00	1.00	0.00
D5	−0.15	−16.13	−14.77	52.00	43.51	45.54	52.00	0.00
D6	−0.82	−2.48	−0.33	9.92	8.74	10.28	10.28	0.00
D7	−2.01	−1.12	−0.03	5.85	6.71	7.11	7.11	0.11
D8	−0.22	−6.41	−7.81	22.26	17.99	17.93	22.26	0.00
D9	−0.85	−16.15	−13.10	61.95	52.64	53.90	61.95	0.00
D10	−2.78	−0.25	−1.05	6.37	8.16	7.29	8.16	0.00
	E1 $((V_1)(4))$	E2 $((V_2)(4))$	E3 $((V_3)(4))$	E1 $((P_1)(4))$	E2 $((P_2)(4))$	E3 $((P_3)(4))$	$((P_{gb})(4))$	$((P_{gb})(t)) - ((P_{gb})(t-1))$
D1	−4.74	−3.93	−0.01	54.10	54.81	56.00	56.00	0.00
D2	−3.17	−2.83	−0.08	26.45	26.79	28.09	28.09	0.00
D3	0.00	0.00	0.00	1.00	1.00	1.00	1.00	0.00
D4	−0.05	−0.12	0.00	0.98	0.96	1.00	1.00	0.00
D5	−0.08	–23.83	−20.95	52.00	43.51	45.54	52.00	0.00
D6	−1.58	−3.64	−0.37	9.92	8.74	10.28	10.28	0.00
D7	−2.94	−1.54	−0.09	5.85	6.71	7.11	7.11	0.00
D8	−0.30	−9.74	−12.60	22.26	17.99	17.93	22.26	0.00
D9	−1.13	–23.32	−20.70	61.95	52.64	53.90	61.95	0.00
D10	−4.08	−0.24	−1.59	6.37	8.16	7.29	8.16	0.00

Table 6
Reward Degrees of Fuzzy Q Relation Matrix Among the Experts.

Expert 1-Expert 2	**CAEMEFF**	**RETINV**	**ENGCAPEX**	**ENVCOMSTD**
CAEMEFF	(0.00, 0.00, 0.00)	(−0.05, 0.03, 0.02)	(−0.05, 0.03, 0.02)	(0.00, 0.00, 0.00)
RETINV	(−0.06, 0.05, 0.02)	(0.00, 0.00, 0.00)	(0.00, 0.00, 0.00)	(0.00, 0.00, 0.00)
ENGCAPEX	(−0.06, 0.05, 0.02)	(−0.06, 0.05, 0.02)	(0.00, 0.00, 0.00)	(−0.05, 0.03, 0.02)
ENVCOMSTD	(0.00, 0.00, 0.00)	(0.00, 0.00, 0.00)	(0.00, 0.00, 0.00)	(0.00, 0.00, 0.00)
Expert 1-Expert 3	**CAEMEFF**	**RETINV**	**ENGCAPEX**	**ENVCOMSTD**
CAEMEFF	(0.00, 0.00, 0.00)	(0.00, 0.00, 0.00)	(0.00, 0.00, 0.00)	(0.00, 0.00, 0.00)
RETINV	(0.05, −0.03, −0.02)	(0.00, 0.00, 0.00)	(0.00, 0.00, 0.00)	(0.00, 0.00, 0.00)
ENGCAPEX	(0.00, 0.00, 0.00)	(0.00, 0.00, 0.00)	(0.00, 0.00, 0.00)	(0.00, 0.00, 0.00)
ENVCOMSTD	(0.07, −0.05, −0.02)	(0.12, −0.08, −0.03)	(0.00, 0.00, 0.00)	(0.00, 0.00, 0.00)

Table 7
Reward Degrees of Fuzzy Q Decision Matrix Among the Experts.

Expert 1-Expert 2	CAEMEFF	RETINV	ENGCAPEX	ENVCOMSTD
SOLAR	(0.00, 0.00, 0.00)	(−0.11, 0.08, 0.03)	(0.00, 0.00, 0.00)	(0.00, 0.00, 0.00)
WIND	(0.00, 0.00, 0.00)	(0.00, 0.00, 0.00)	(0.00, 0.00, 0.00)	(−0.06, 0.05, 0.02)
GEOTHERMAL	(−0.11, 0.08, 0.03)	(0.00, 0.00, 0.00)	(0.00, 0.00, 0.00)	(0.00, 0.00, 0.00)
BIOMASS	(0.00, 0.00, 0.00)	(0.00, 0.00, 0.00)	(0.00, 0.00, 0.00)	(0.00, 0.00, 0.00)
HYDROPOWER	(0.00, 0.00, 0.00)	(0.00, 0.00, 0.00)	(0.00, 0.00, 0.00)	(−0.06, 0.05, 0.02)
Expert 1-Expert 3	**CAEMEFF**	**RETINV**	**ENGCAPEX**	**ENVCOMSTD**
SOLAR	(0.00, 0.00, 0.00)	(−0.05, 0.03, 0.02)	(0.00, 0.00, 0.00)	(0.00, 0.00, 0.00)
WIND	(0.00, 0.00, 0.00)	(0.00, 0.00, 0.00)	(0.00, 0.00, 0.00)	(0.00, 0.00, 0.00)
GEOTHERMAL	(0.00, 0.00, 0.00)	(0.00, 0.00, 0.00)	(0.00, 0.00, 0.00)	(0.00, 0.00, 0.00)
BIOMASS	(−0.05, 0.03, 0.02)	(−0.05, 0.03, 0.02)	(0.00, 0.00, 0.00)	(−0.05, 0.03, 0.02)
HYDROPOWER	(−0.05, 0.03, 0.02)	(−0.05, 0.03, 0.02)	(0.00, 0.00, 0.00)	(0.00, 0.00, 0.00)

Table 8
Penalty Degrees of Fuzzy Q Relation Matrix Among the Experts.

Expert 1-Expert 2	CAEMEFF	RETINV	ENGCAPEX	ENVCOMSTD
CAEMEFF	(0.00, 0.00, 0.00)	(0.05, −0.03, −0.02)	(0.05, −0.03, −0.02)	(0.00, 0.00, 0.00)
RETINV	(0.07, −0.05, −0.02)	(0.00, 0.00, 0.00)	(0.00, 0.00, 0.00)	(0.00, 0.00, 0.00)
ENGCAPEX	(0.07, −0.05, −0.02)	(0.07, −0.05, −0.02)	(0.00, 0.00, 0.00)	(0.05, −0.03, −0.02)
ENVCOMSTD	(0.00, 0.00, 0.00)	(0.00, 0.00, 0.00)	(0.00, 0.00, 0.00)	(0.00, 0.00, 0.00)
Expert 1-Expert 3	**CAEMEFF**	**RETINV**	**ENGCAPEX**	**ENVCOMSTD**
CAEMEFF	(0.00, 0.00, 0.00)	(0.00, 0.00, 0.00)	(0.00, 0.00, 0.00)	(0.00, 0.00, 0.00)
RETINV	(−0.05, 0.03, 0.02)	(0.00, 0.00, 0.00)	(0.00, 0.00, 0.00)	(0.00, 0.00, 0.00)
ENGCAPEX	(0.00, 0.00, 0.00)	(0.00, 0.00, 0.00)	(0.00, 0.00, 0.00)	(0.00, 0.00, 0.00)
ENVCOMSTD	(−0.07, 0.05, 0.02)	(−0.12, 0.09, 0.03)	(0.00, 0.00, 0.00)	(0.00, 0.00, 0.00)

Table 9
Penalty Degrees of Fuzzy Q Decision Matrix Among the Experts.

Expert 1-Expert 2	CAEMEFF	RETINV	ENGCAPEX	ENVCOMSTD
SOLAR	(0.00, 0.00, 0.00)	(0.12,-0.09,-0.03)	(0.00, 0.00, 0.00)	(0.00, 0.00, 0.00)
WIND	(0.00, 0.00, 0.00)	(0.00, 0.00, 0.00)	(0.00, 0.00, 0.00)	(0.07,-0.05,-0.02)
GEOTHERMAL	(0.12,-0.09,-0.03)	(0.00, 0.00, 0.00)	(0.00, 0.00, 0.00)	(0.00, 0.00, 0.00)
BIOMASS	(0.00, 0.00, 0.00)	(0.00, 0.00, 0.00)	(0.00, 0.00, 0.00)	(0.00, 0.00, 0.00)
HYDROPOWER	(0.00, 0.00, 0.00)	(0.00, 0.00, 0.00)	(0.00, 0.00, 0.00)	(0.07,-0.05,-0.02)
Expert 1-Expert 3	**CAEMEFF**	**RETINV**	**ENGCAPEX**	**ENVCOMSTD**
SOLAR	(0.00, 0.00, 0.00)	(0.05, −0.03, −0.02)	(0.00, 0.00, 0.00)	(0.00, 0.00, 0.00)
WIND	(0.00, 0.00, 0.00)	(0.00, 0.00, 0.00)	(0.00, 0.00, 0.00)	(0.00, 0.00, 0.00)
GEOTHERMAL	(0.00, 0.00, 0.00)	(0.00, 0.00, 0.00)	(0.00, 0.00, 0.00)	(0.00, 0.00, 0.00)
BIOMASS	(0.05, −0.03, −0.02)	(0.05, −0.03, −0.02)	(0.00, 0.00, 0.00)	(0.05, −0.03, −0.02)
HYDROPOWER	(0.05, −0.03, −0.02)	(0.05, −0.03, −0.02)	(0.00, 0.00, 0.00)	(0.00, 0.00, 0.00)

3.2. *Weighting the criteria with molecular fuzzy cognitive maps*

The values in Table 16 expressed by Equation (26) are used to calculate the weights of the criteria. Afterwards, the average fuzzy Q values of the relation matrix is computed with the help of Equation (27). The result is detailed in Table 18.

In the next step of molecular fuzzy cognitive maps method, the fuzzy vectors for relation matrix are defined using Equation (28). These fuzzy vectors are shared in Table 19.

Then, the $(u_i.u_j)$ for the pair-wise comparison of the criteria is computed by Equation (29), and the results of computation are illustrated in Table 20.

Using the dot products, the cosine of angle between the fuzzy relation vectors is calculated with Equation (30). The values of cosine function are shown in Table 21.

Using Equation (31), the angle in radians for relation matrix is obtained. The angles are given in Table 22.

With the help of Equations (32)-(37), the normalize process is performed. Normalize the angle relation matrix using various molecular geometry shapes are summarized in Table 23.

Table 10
Updated Values of Fuzzy Q Relation Matrix Among the Experts.

Expert 1-Expert 2	CAEMEFF	RETINV	ENGCAPEX	ENVCOMSTD
CAEMEFF	(0.00, 0.00, 0.00)	(0.94, 0.06, 0.00)	(0.94, 0.06, 0.00)	(0.80, 0.15, 0.05)
RETINV	(0.79, 0.16, 0.05)	(0.00, 0.00, 0.00)	(0.95, 0.05, 0.00)	(0.95, 0.05, 0.00)
ENGCAPEX	(0.79, 0.16, 0.05)	(0.79, 0.16, 0.05)	(0.00, 0.00, 0.00)	(0.94, 0.06, 0.00)
ENVCOMSTD	(0.60, 0.30, 0.10)	(0.60, 0.30, 0.10)	(0.95, 0.05, 0.00)	(0.00, 0.00, 0.00)
Expert 1-Expert 3	**CAEMEFF**	**RETINV**	**ENGCAPEX**	**ENVCOMSTD**
CAEMEFF	(0.00, 0.00, 0.00)	(0.95, 0.05, 0.00)	(0.95, 0.05, 0.00)	(0.80, 0.15, 0.05)
RETINV	(0.81, 0.14, 0.05)	(0.00, 0.00, 0.00)	(0.95, 0.05, 0.00)	(0.95, 0.05, 0.00)
ENGCAPEX	(0.80, 0.15, 0.05)	(0.80, 0.15, 0.05)	(0.00, 0.00, 0.00)	(0.95, 0.05, 0.00)
ENVCOMSTD	(0.61, 0.29, 0.10)	(0.62, 0.28, 0.09)	(0.95, 0.05, 0.00)	(0.00, 0.00, 0.00)

Table 11
Updated Values of Fuzzy Q Decision Matrix Among the Experts.

Expert 1-Expert 2	CAEMEFF	RETINV	ENGCAPEX	ENVCOMSTD
SOLAR	(0.80, 0.15, 0.05)	(0.93, 0.07, 0.01)	(0.80, 0.15, 0.05)	(0.80, 0.15, 0.05)
WIND	(0.80, 0.15, 0.05)	(0.80, 0.15, 0.05)	(0.95, 0.05, 0.00)	(0.79, 0.16, 0.05)
GEOTHERMAL	(0.93, 0.07, 0.01)	(0.95, 0.05, 0.00)	(0.95, 0.05, 0.00)	(0.80, 0.15, 0.05)
BIOMASS	(0.95, 0.05, 0.00)	(0.95, 0.05, 0.00)	(0.80, 0.15, 0.05)	(0.95, 0.05, 0.00)
HYDROPOWER	(0.95, 0.05, 0.00)	(0.95, 0.05, 0.00)	(0.95, 0.05, 0.00)	(0.79, 0.16, 0.05)
Expert 1-Expert 3	**CAEMEFF**	**RETINV**	**ENGCAPEX**	**ENVCOMSTD**
SOLAR	(0.80, 0.15, 0.05)	(0.94, 0.06, 0.00)	(0.80, 0.15, 0.05)	(0.80, 0.15, 0.05)
WIND	(0.80, 0.15, 0.05)	(0.80, 0.15, 0.05)	(0.95, 0.05, 0.00)	(0.80, 0.15, 0.05)
GEOTHERMAL	(0.95, 0.05, 0.00)	(0.95, 0.05, 0.00)	(0.95, 0.05, 0.00)	(0.80, 0.15, 0.05)
BIOMASS	(0.94, 0.06, 0.00)	(0.94, 0.06, 0.00)	(0.80, 0.15, 0.05)	(0.94, 0.06, 0.00)
HYDROPOWER	(0.94, 0.06, 0.00)	(0.94, 0.06, 0.00)	(0.95, 0.05, 0.00)	(0.80, 0.15, 0.05)

Table 12
Absolute Difference of Fuzzy Q Relation Matrix Among the Experts (Iteration 1).

Expert 1-Expert 2	CAEMEFF	RETINV	ENGCAPEX	ENVCOMSTD
CAEMEFF	(0.000,.000,.000)	(0.010,.007,.003)	(0.010,.007,.003)	(0.000,.000,.000)
RETINV	(0.013,.010,.003)	(0.000,.000,.000)	(0.000,.000,.000)	(0.000,.000,.000)
ENGCAPEX	(0.013,.010,.003)	(0.013,.010,.003)	(0.000,.000,.000)	(0.010,.007,.003)
ENVCOMSTD	(0.000,.000,.000)	(0.000,.000,.000)	(0.000,.000,.000)	(0.000,.000,.000)
Expert 1-Expert 3	**CAEMEFF**	**RETINV**	**ENGCAPEX**	**ENVCOMSTD**
CAEMEFF	(0.000,.000,.000)	(0.000,.000,.000)	(0.000,.000,.000)	(0.000,.000,.000)
RETINV	(0.010,.007,.003)	(0.000,.000,.000)	(0.000,.000,.000)	(0.000,.000,.000)
ENGCAPEX	(0.000,.000,.000)	(0.000,.000,.000)	(0.000,.000,.000)	(0.000,.000,.000)
ENVCOMSTD	(0.014,.010,.003)	(0.024,.017,.007)	(0.000,.000,.000)	(0.000,.000,.000)

For linear shape, the $recip\left(\theta_{u_i,u_j}\right)$ values are estimated by Equation (38). The result for linear shape of molecular geometry shapes is shared in Table 24.

Next, Equations (39) and (40) presents the information about the normalized relation matrix for linear shape. The matrix is displayed in Table 25.

Finally, the state vector and the function values iteratively as well as the weights of the criteria are calculated using Equations (41)-(44). The details of result for linear shape are tabulated in Table 26.

According to Table 26, the results of the sixth and fifth iterations are the same. Therefore, it is seen that the final weighting priorities of the criteria are obtained. As can be seen from Table 26, the most important and effective criterion is energy capacity expansion for the corporate environmental performance with renewable energy investments. Comparative prioritization results of the criteria by the various molecular geometry shapes and learning rate are found. The comparative result is summarized in Table 27.

According to Table 27, the priority results calculated with five different molecular geometry shapes are similar. In addition, it can be said that the analysis is consistent according to the results obtained with different learning rates.

Table 13
Absolute Difference of Fuzzy Q Decision Matrix Among the Experts (Iteration 1).

Expert 1-Expert 2	CAEMEFF	RETINV	ENGCAPEX	ENVCOMSTD
SOLAR	(0.000,.000,.000)	(0.023,.017,.007)	(0.000,.000,.000)	(0.000,.000,.000)
WIND	(0.000,.000,.000)	(0.000,.000,.000)	(0.000,.000,.000)	(0.013,.010,.003)
GEOTHERMAL	(0.023,.017,.007)	(0.000,.000,.000)	(0.000,.000,.000)	(0.000,.000,.000)
BIOMASS	(0.000,.000,.000)	(0.000,.000,.000)	(0.000,.000,.000)	(0.000,.000,.000)
HYDROPOWER	(0.000,.000,.000)	(0.000,.000,.000)	(0.000,.000,.000)	(0.013,.010,.003)
Expert 1-Expert 3	**CAEMEFF**	**RETINV**	**ENGCAPEX**	**ENVCOMSTD**
SOLAR	(0.000,.000,.000)	(0.010,.007,.003)	(0.000,.000,.000)	(0.000,.000,.000)
WIND	(0.000,.000,.000)	(0.000,.000,.000)	(0.000,.000,.000)	(0.000,.000,.000)
GEOTHERMAL	(0.000,.000,.000)	(0.000,.000,.000)	(0.000,.000,.000)	(0.000,.000,.000)
BIOMASS	(0.010,.007,.003)	(0.010,.007,.003)	(0.000,.000,.000)	(0.010,.007,.003)
HYDROPOWER	(0.010,.007,.003)	(0.010,.007,.003)	(0.000,.000,.000)	(0.000,.000,.000)

Table 14
Iterative Absolute Differences of Fuzzy Relation Matrix Among Expert 1 And Expert 3.

Second Iteration				
Expert 1-Expert 3	**CAEMEFF**	**RETINV**	**ENGCAPEX**	**ENVCOMSTD**
CAEMEFF	(0.000,.000,.000)	(0.000,.000,.000)	(0.000,.000,.000)	(0.000,.000,.000)
RETINV	(0.009,.006,.003)	(0.000,.000,.000)	(0.000,.000,.000)	(0.000,.000,.000)
ENGCAPEX	(0.000,.000,.000)	(0.000,.000,.000)	(0.000,.000,.000)	(0.000,.000,.000)
ENVCOMSTD	(0.013,.009,.003)	(0.022,.016,.006)	(0.000,.000,.000)	(0.000,.000,.000)
Third Iteration				
Expert 1-Expert 3	**CAEMEFF**	**RETINV**	**ENGCAPEX**	**ENVCOMSTD**
CAEMEFF	(0.000,.000,.000)	(0.000,.000,.000)	(0.000,.000,.000)	(0.000,.000,.000)
RETINV	(0.009,.006,.003)	(0.000,.000,.000)	(0.000,.000,.000)	(0.000,.000,.000)
ENGCAPEX	(0.000,.000,.000)	(0.000,.000,.000)	(0.000,.000,.000)	(0.000,.000,.000)
ENVCOMSTD	(0.012,.009,.003)	(0.021,.015,.006)	(0.000,.000,.000)	(0.000,.000,.000)
Fourth Iteration				
Expert 1-Expert 3	**CAEMEFF**	**RETINV**	**ENGCAPEX**	**ENVCOMSTD**
CAEMEFF	(0.000,.000,.000)	(0.000,.000,.000)	(0.000,.000,.000)	(0.000,.000,.000)
RETINV	(0.008,.006,.003)	(0.000,.000,.000)	(0.000,.000,.000)	(0.000,.000,.000)
ENGCAPEX	(0.000,.000,.000)	(0.000,.000,.000)	(0.000,.000,.000)	(0.000,.000,.000)
ENVCOMSTD	(0.011,.008,.003)	(0.019,.014,.006)	(0.000,.000,.000)	(0.000,.000,.000)

3.3. Ranking the alternatives with fuzzy molecular ranking (MORAN)

The values in Table 17 expressed by Equation (45) are used to rank of the alternatives. Solar, wind, geothermal, biomass and hydropower are defined as five different renewable energy alternatives. Afterwards, the average fuzzy values of the decision matrix are calculated by Equation (27). The result is reported in Table 28.

After that, using weights and Equation (46), the weighted decision matrix is created. The matrix is shared in Table 29.

The y_i for decision matrix is defined with the help of Equation (47) and summarized in Table 30.

By Equation (48), the dot products of y_i for the decision matrix are computed. The dot products are given in Table 31.

Equation (49) gives information about the cosine values. The cosine of angle between the fuzzy decision vectors is shared in Table 32.

Afterwards, the angle in radians for decision matrix is computed with the help of Equation (50). The results are detailed in Table 33.

These values are normalized using different molecular geometry shapes. Using Equations (51)-(56), the normalized values are illustrated in Table 34.

After estimating different normalized values, reciprocal values are computed with the help of Equation (57) for linear shape. The reciprocal values of normalized values are displayed in Table 35.

With the help of Equation (58), the final decision matrix is constructed, and Equation (59) calculates the aggregated values. The ranking result for linear shape is given in Table 36.

According to the results in Table 36, the most suitable renewable energy type is geothermal. Comparative ranking results of the renewable energy types by the different molecular geometry shapes and learning rates are found. The results are shown in Table 37.

While the results obtained with the learning rate are consistent, it is seen in Table 37 that the ranking results calculated for different

Table 15
Iterative Absolute Differences of Fuzzy Decision Matrix Among Expert 1 And Expert 2.

Second Iteration				
Expert 1-Expert 2	**CAEMEFF**	**RETINV**	**ENGCAPEX**	**ENVCOMSTD**
SOLAR	(0.000,.000,.000)	(0.022,.016,.006)	(0.000,.000,.000)	(0.000,.000,.000)
WIND	(0.000,.000,.000)	(0.000,.000,.000)	(0.000,.000,.000)	(0.012,.009,.003)
GEOTHERMAL	(0.022,.016,.006)	(0.000,.000,.000)	(0.000,.000,.000)	(0.000,.000,.000)
BIOMASS	(0.000,.000,.000)	(0.000,.000,.000)	(0.000,.000,.000)	(0.000,.000,.000)
HYDROPOWER	(0.000,.000,.000)	(0.000,.000,.000)	(0.000,.000,.000)	(0.012,.009,.003)
Third Iteration				
Expert 1-Expert 2	**CAEMEFF**	**RETINV**	**ENGCAPEX**	**ENVCOMSTD**
SOLAR	(0.000,.000,.000)	(0.020,.015,.006)	(0.000,.000,.000)	(0.000,.000,.000)
WIND	(0.000,.000,.000)	(0.000,.000,.000)	(0.000,.000,.000)	(0.012,.009,.003)
GEOTHERMAL	(0.020,.015,.006)	(0.000,.000,.000)	(0.000,.000,.000)	(0.000,.000,.000)
BIOMASS	(0.000,.000,.000)	(0.000,.000,.000)	(0.000,.000,.000)	(0.000,.000,.000)
HYDROPOWER	(0.000,.000,.000)	(0.000,.000,.000)	(0.000,.000,.000)	(0.012,.009,.003)
Fourth Iteration				
Expert 1-Expert 2	**CAEMEFF**	**RETINV**	**ENGCAPEX**	**ENVCOMSTD**
SOLAR	(0.000,.000,.000)	(0.019,.014,.005)	(0.000,.000,.000)	(0.000,.000,.000)
WIND	(0.000,.000,.000)	(0.000,.000,.000)	(0.000,.000,.000)	(0.011,.008,.003)
GEOTHERMAL	(0.019,.014,.005)	(0.000,.000,.000)	(0.000,.000,.000)	(0.000,.000,.000)
BIOMASS	(0.000,.000,.000)	(0.000,.000,.000)	(0.000,.000,.000)	(0.000,.000,.000)
HYDROPOWER	(0.000,.000,.000)	(0.000,.000,.000)	(0.000,.000,.000)	(0.011,.008,.003)

Table 16
Fuzzy Q Values for Relation Matrix by The Experts.

Expert 1(initial Q matrix)	**CAEMEFF**	**RETINV**	**ENGCAPEX**	**ENVCOMSTD**
CAEMEFF	(0.00, 0.00, 0.00)	(0.95, 0.05, 0.00)	(0.95, 0.05, 0.00)	(0.80, 0.15, 0.05)
RETINV	(0.80, 0.15, 0.05)	(0.00, 0.00, 0.00)	(0.95, 0.05, 0.00)	(0.95, 0.05, 0.00)
ENGCAPEX	(0.80, 0.15, 0.05)	(0.80, 0.15, 0.05)	(0.00, 0.00, 0.00)	(0.95, 0.05, 0.00)
ENVCOMSTD	(0.60, 0.30, 0.10)	(0.60, 0.30, 0.10)	(0.95, 0.05, 0.00)	(0.00, 0.00, 0.00)
Expert 2 (Balanced Q matrix)	**CAEMEFF**	**RETINV**	**ENGCAPEX**	**ENVCOMSTD**
CAEMEFF	(0.00, 0.00, 0.00)	(0.94, 0.06, 0.00)	(0.94, 0.06, 0.00)	(0.80, 0.15, 0.05)
RETINV	(0.79, 0.16, 0.05)	(0.00, 0.00, 0.00)	(0.95, 0.05, 0.00)	(0.95, 0.05, 0.00)
ENGCAPEX	(0.79, 0.16, 0.05)	(0.79, 0.16, 0.05)	(0.00, 0.00, 0.00)	(0.94, 0.06, 0.00)
ENVCOMSTD	(0.60, 0.30, 0.10)	(0.60, 0.30, 0.10)	(0.95, 0.05, 0.00)	(0.00, 0.00, 0.00)
Expert 3 (Balanced Q matrix)	**CAEMEFF**	**RETINV**	**ENGCAPEX**	**ENVCOMSTD**
CAEMEFF	(0.00, 0.00, 0.00)	(0.95, 0.05, 0.00)	(0.95, 0.05, 0.00)	(0.80, 0.15, 0.05)
RETINV	(0.84, 0.13, 0.04)	(0.00, 0.00, 0.00)	(0.95, 0.05, 0.00)	(0.95, 0.05, 0.00)
ENGCAPEX	(0.80, 0.15, 0.05)	(0.80, 0.15, 0.05)	(0.00, 0.00, 0.00)	(0.95, 0.05, 0.00)
ENVCOMSTD	(0.65, 0.26, 0.09)	(0.69, 0.24, 0.08)	(0.95, 0.05, 0.00)	(0.00, 0.00, 0.00)

molecular geometric shapes are the same. Under all conditions and situations, geothermal is the best type of renewable energy.

To further mitigate subjective influences, a sensitivity analysis was conducted across various molecular geometry shapes—linear, trigonal planar, tetrahedral, trigonal bipyramidal, and octahedral. The analysis consistently confirmed stability in prioritization results across these shapes, as shown for weighting in Tables 24–27 and ranking in Tables 34-37, validating that the findings are resilient to variations in decision matrix normalization methods. This methodical approach not only enhances the study's objectivity but also reinforces the reliability of criteria weighting and alternative ranking results. By employing these advanced computational techniques, the study minimizes bias impacts and bolsters confidence in the decision-making process outcomes.

Also, the sensitivity analysis underscores financial stability and customer satisfaction as the most influential criteria in ranking alternatives. These findings indicate that even minor adjustments in these criteria substantially impact the preference order, particularly for solar (A1) and wind energy (A2). Notably, solar (A1) retained a high ranking across varied weights, while bioenergy (A3) showed notable sensitivity, especially to changes in customer satisfaction (C2). This suggests that solar provides a more stable and reliable investment under diverse conditions. We recommend prioritizing resources towards financial planning and customer engagement to enhance decision robustness, as well as ongoing monitoring for scenarios where bioenergy could become favourable.

Table 17
Fuzzy Q Values for Decision Matrix by The Experts.

Expert 1(initial Q matrix)	CAEMEFF	RETINV	ENGCAPEX	ENVCOMSTD
SOLAR	(0.80, 0.15, 0.05)	(0.95, 0.05, 0.00)	(0.80, 0.15, 0.05)	(0.80, 0.15, 0.05)
WIND	(0.80, 0.15, 0.05)	(0.80, 0.15, 0.05)	(0.95, 0.05, 0.00)	(0.80, 0.15, 0.05)
GEOTHERMAL	(0.95, 0.05, 0.00)	(0.95, 0.05, 0.00)	(0.95, 0.05, 0.00)	(0.80, 0.15, 0.05)
BIOMASS	(0.95, 0.05, 0.00)	(0.95, 0.05, 0.00)	(0.80, 0.15, 0.05)	(0.95, 0.05, 0.00)
HYDROPOWER	(0.95, 0.05, 0.00)	(0.95, 0.05, 0.00)	(0.95, 0.05, 0.00)	(0.80, 0.15, 0.05)
Expert 2 (Balanced Q matrix)	**CAEMEFF**	**RETINV**	**ENGCAPEX**	**ENVCOMSTD**
SOLAR	(0.80, 0.15, 0.05)	(0.87, 0.11, 0.02)	(0.80, 0.15, 0.05)	(0.80, 0.15, 0.05)
WIND	(0.80, 0.15, 0.05)	(0.80, 0.15, 0.05)	(0.95, 0.05, 0.00)	(0.75, 0.19, 0.06)
GEOTHERMAL	(0.87, 0.11, 0.02)	(0.95, 0.05, 0.00)	(0.95, 0.05, 0.00)	(0.80, 0.15, 0.05)
BIOMASS	(0.95, 0.05, 0.00)	(0.95, 0.05, 0.00)	(0.80, 0.15, 0.05)	(0.95, 0.05, 0.00)
HYDROPOWER	(0.95, 0.05, 0.00)	(0.95, 0.05, 0.00)	(0.95, 0.05, 0.00)	(0.75, 0.19, 0.06)
Expert 3 (Balanced Q matrix)	**CAEMEFF**	**RETINV**	**ENGCAPEX**	**ENVCOMSTD**
SOLAR	(0.80, 0.15, 0.05)	(0.94, 0.06, 0.00)	(0.80, 0.15, 0.05)	(0.80, 0.15, 0.05)
WIND	(0.80, 0.15, 0.05)	(0.80, 0.15, 0.05)	(0.95, 0.05, 0.00)	(0.80, 0.15, 0.05)
GEOTHERMAL	(0.95, 0.05, 0.00)	(0.95, 0.05, 0.00)	(0.95, 0.05, 0.00)	(0.80, 0.15, 0.05)
BIOMASS	(0.94, 0.06, 0.00)	(0.94, 0.06, 0.00)	(0.80, 0.15, 0.05)	(0.94, 0.06, 0.00)
HYDROPOWER	(0.94, 0.06, 0.00)	(0.94, 0.06, 0.00)	(0.95, 0.05, 0.00)	(0.80, 0.15, 0.05)

Table 18
Averaged Fuzzy Numbers for Relation Matrix.

	CAEMEFF	RETINV	ENGCAPEX	ENVCOMSTD
CAEMEFF	(0.00, 0.00, 0.00)	(0.95, 0.05, 0.00)	(0.95, 0.05, 0.00)	(0.80, 0.15, 0.05)
RETINV	(0.81, 0.15, 0.05)	(0.00, 0.00, 0.00)	(0.95, 0.05, 0.00)	(0.95, 0.05, 0.00)
ENGCAPEX	(0.80, 0.15, 0.05)	(0.80, 0.15, 0.05)	(0.00, 0.00, 0.00)	(0.95, 0.05, 0.00)
ENVCOMSTD	(0.62, 0.29, 0.10)	(0.63, 0.28, 0.09)	(0.95, 0.05, 0.00)	(0.00, 0.00, 0.00)

Table 19
Fuzzy Vectors for Relation Matrix.

Vectors	Fuzzy Vectors (excluding self-connections)
u_1	[(0.95, 0.05, 0.00), (0.95, 0.05, 0.00), (0.80, 0.15, 0.05)]
u_2	[(0.81, 0.15, 0.05), (0.95, 0.05, 0.00), (0.95, 0.05, 0.00)]
u_3	[(0.80, 0.15, 0.05), (0.80, 0.15, 0.05), (0.95, 0.05, 0.00)]
u_4	[(0.62, 0.29, 0.10), (0.63, 0.28, 0.09), (0.95, 0.05, 0.00)]

Table 20
Dot Products of Fuzzy Relation Vectors.

	$\boldsymbol{u}_1$	$\boldsymbol{u}_2$	$\boldsymbol{u}_3$	$\boldsymbol{u}_4$
u_1		2.442	2.288	1.976
u_2	2.442		2.333	2.060
u_3	2.288	2.333		1.989
u_4	1.976	2.060	1.989	

Table 21
Cosine of Angle Between Fuzzy Relation Vectors.

	$\cos(\boldsymbol{\theta}_{\boldsymbol{u}_1})$	$\cos(\boldsymbol{\theta}_{\boldsymbol{u}_2})$	$\cos(\boldsymbol{\theta}_{\boldsymbol{u}_3})$	$\cos(\boldsymbol{\theta}_{\boldsymbol{u}_4})$
$\cos(\theta_{u_1})$		0.987	0.979	0.924
$\cos(\theta_{u_2})$	0.987		0.994	0.959
$\cos(\theta_{u_3})$	0.979	0.994		0.980
$\cos(\theta_{u_4})$	0.924	0.959	0.980	

Table 22
Angle In Radians for Relation Matrix.

	θ_{u_1}	θ_{u_2}	θ_{u_3}	θ_{u_4}
θ_{u_1}		0.162	0.205	0.394
θ_{u_2}	0.162		0.113	0.289
θ_{u_3}	0.205	0.113		0.201
θ_{u_4}	0.394	0.289	0.201	

Table 23
Normalized Angle Relation Values Using Various Molecular Geometry Shapes.

Linear	$norm(\theta_{u_1})$	$norm(\theta_{u_2})$	$norm(\theta_{u_3})$	$norm(\theta_{u_4})$
$norm(\theta_{u_1})$	0.000	0.052	0.065	0.125
$norm(\theta_{u_2})$	0.052	0.000	0.036	0.092
$norm(\theta_{u_3})$	0.065	0.036	0.000	0.064
$norm(\theta_{u_4})$	0.125	0.092	0.064	0.000
Trigonal Planar	$norm(\theta_{u_1})$	$norm(\theta_{u_2})$	$norm(\theta_{u_3})$	$norm(\theta_{u_4})$
$norm(\theta_{u_1})$	0.000	0.077	0.098	0.188
$norm(\theta_{u_2})$	0.077	0.000	0.054	0.138
$norm(\theta_{u_3})$	0.098	0.054	0.000	0.096
$norm(\theta_{u_4})$	0.188	0.138	0.096	0.000
Tetrahedral	$norm(\theta_{u_1})$	$norm(\theta_{u_2})$	$norm(\theta_{u_3})$	$norm(\theta_{u_4})$
$norm(\theta_{u_1})$	0.000	0.085	0.107	0.206
$norm(\theta_{u_2})$	0.085	0.000	0.059	0.151
$norm(\theta_{u_3})$	0.107	0.059	0.000	0.105
$norm(\theta_{u_4})$	0.206	0.151	0.105	0.000
Trigonal Bipyramidal	$norm(\theta_{u_1})$	$norm(\theta_{u_2})$	$norm(\theta_{u_3})$	$norm(\theta_{u_4})$
$norm(\theta_{u_1})$	0.000	0.089	0.112	0.215
$norm(\theta_{u_2})$	0.089	0.000	0.062	0.158
$norm(\theta_{u_3})$	0.112	0.062	0.000	0.110
$norm(\theta_{u_4})$	0.215	0.158	0.110	0.000
Octahedral	$norm(\theta_{u_1})$	$norm(\theta_{u_2})$	$norm(\theta_{u_3})$	$norm(\theta_{u_4})$
$norm(\theta_{u_1})$	0.000	0.103	0.131	0.251
$norm(\theta_{u_2})$	0.103	0.000	0.072	0.184
$norm(\theta_{u_3})$	0.131	0.072	0.000	0.128
$norm(\theta_{u_4})$	0.251	0.184	0.128	0.000

Table 24
Reciprocal Values of The Normalized Angles.

	$\frac{1}{norm(\theta_{u_1})}$	$\frac{1}{norm(\theta_{u_2})}$	$\frac{1}{norm(\theta_{u_3})}$	$\frac{1}{norm(\theta_{u_4})}$
$\frac{1}{norm(\theta_{u_1})}$		19.363	15.304	7.982
$\frac{1}{norm(\theta_{u_2})}$	19.363		27.912	10.871
$\frac{1}{norm(\theta_{u_3})}$	15.304	27.912		15.618
$\frac{1}{norm(\theta_{u_4})}$	7.982	10.871	15.618	

4. Discussion

Energy capacity expansion plays the most important role in improving the environmental performance of businesses. More emphasis should be placed on renewable energy projects to expand capacity. This has some advantages for both businesses and countries. Preferring renewable energy over fossil fuels allows for a reduction in environmental pollution. [25] discussed that reducing carbon emissions also supports a more successful fight against climate change. On the other hand, increasing capacity is of critical

Table 25
Normalized Relation Matrix.

	CAEMEFF	RETINV	ENGCAPEX	ENVCOMSTD
CAEMEFF	0	0.200	0.158	0.082
RETINV	0.200	0	0.288	0.112
ENGCAPEX	0.158	0.288	0	0.161
ENVCOMSTD	0.082	0.112	0.161	0

importance in ensuring energy security. According to [26], with the development of renewable energy projects, countries can produce the energy they need themselves. This makes a significant contribution to ensuring energy independence. In other words, thanks to these projects, countries can reduce their dependence on other countries for energy. This allows energy efficiency to be increased even further. In this way, the environmental performance of projects can also increase significantly [27].

Return on investment is another factor that plays an important role in improving environmental performance. The high level of these revenues shows that projects can also create economic value. Investors show more interest in projects with high financial performance. Similarly, financial institutions are more willing to provide loans to these projects. [28] denoted that projects with high financial success can more easily access the funds they need. [29] demonstrated considering that the initial investment costs in energy projects are also very high, this situation is of critical importance for the development of projects. [30] identified that businesses with high return on investment can also be more successful in risk management. Businesses with high financial performance can manage liquidity more effectively. [31] concluded that businesses can pay their debts on time. Similarly, businesses with high financial performance can also effectively manage exchange rate risk. This situation allows possible financial losses to be minimized.

In many different studies, the issue of energy capacity expansion comes to the fore in increasing the environmental performance of renewable energy projects. On the other hand, the model proposed in this study differs from many other models. Most studies in the literature are analyzed with classical fuzzy logic or traditional fuzzy sets [32,33], and [34]. However, in this study, molecular fuzzy sets created by combining molecular geometry and fuzzy logic are used. With the help of this issue, it is possible to reduce the uncertainty in more complex and sensitive decision processes. This situation supports the increase of the efficiency and reliability of the studies. On the other hand, q-learning algorithm and MOPSO techniques are integrated in this study to calculate expert weights. In a significant part of the previous studies, expert opinions are determined with fixed weighting methods [35,36], and [37]. In the proposed model, weights are calculated dynamically using artificial intelligence-based optimization techniques. Furthermore, MORAN is used to rank renewable energy alternatives. Since the MORAN technique performs analysis based on molecular geometry, it provides more sensitive results in multi-criteria decision processes compared to other similar techniques [38,39], and [40].

5. Conclusion

5.1. *Concluding issues*

This study tries to identify the most convenient investment strategies to increase the environmental performance of renewable energy projects. In the first stage, the balanced expert dataset is generated via Q-learning algorithm and multi-objective particle swarm optimization. Secondly, selected criteria are weighted with molecular fuzzy cognitive maps approach. The final stage consists of ranking the alternatives with fuzzy MORAN. The findings denote that energy capacity expansion plays the most important role in improving the environmental performance of businesses. Return on investment is another factor that plays an important role in increasing this performance. Geothermal and hydropower are found as the most successful renewable energy types regarding environmental performance improvement.

The contribution of this study to the literature is to define the most appropriate investment strategies to increase the environmental performance of these projects by generating a new decision-making model. Integrating molecular geometry into decision-making processes increases both the originality and effectiveness of the model. Thus, it is possible to calculate the degrees with a more scientific infrastructure. Integrating Q-learning and swarm optimization techniques into the decision-making model also increases the superiority of the model. In this context, the optimization technique is used to obtain the importance weights of the experts. The most important limitation of this proposed model is the limited data set. The expert opinions used in the study may be limited to a certain area of expertise. This may negatively affect the consistency of the results. In this context, opinions from more experts can be obtained in future studies. In this case, it is possible for the results obtained to be reliable. The use of advanced methods such as Q-learning and molecular fuzzy cognitive maps makes the model quite complex. This situation limits the applicability of the model to every sector. In this context, different conditions should be taken into consideration in the models to be created in the future.

5.2. *Policy applications*

Various policy applications and strategies can be determined to ensure the increase of renewable energy capacity. Carbon tax is an important application in this process. In this context, taxation is carried out to reduce carbon emissions. In this process, more taxation is applied to businesses that use fossil fuels. As a result, fossil fuels lose their competitive advantage to a significant extent since they are more expensive compared to renewable energy projects. This situation allows renewable energy projects to be used more. Similarly, research and development funds can be established to encourage innovations in renewable energy technologies. Thanks to these funds,

Table 26
Iterative State Vector and The Function Values.

	$\boldsymbol{A}(0)$	$\boldsymbol{A}(1)$	$\boldsymbol{f}(\boldsymbol{A}(1))$	$\boldsymbol{A}(2)$	$\boldsymbol{f}(\boldsymbol{A}(2))$	$\boldsymbol{A}(3)$	$\boldsymbol{f}(\boldsymbol{A}(3))$	$\boldsymbol{A}(4)$	$\boldsymbol{f}(\boldsymbol{A}(4))$	$\boldsymbol{A}(5)$	$\boldsymbol{f}(\boldsymbol{A}(5))$	$\boldsymbol{A}(6)$	$\boldsymbol{f}(\boldsymbol{A}(6))$	**Weights**
CAEMEFF	1.000	0.439	0.608	0.279	0.569	0.257	0.564	0.255	0.563	0.254	0.563	0.254	0.563	0.2465
RETINV	1.000	0.599	0.645	0.373	0.592	0.346	0.586	0.343	0.585	0.343	0.585	0.343	0.585	0.2559
ENGCAPEX	1.000	0.606	0.647	0.376	0.593	0.350	0.587	0.346	0.586	0.346	0.586	0.346	0.586	0.2563
ENVCOMSTD	1.000	0.355	0.588	0.226	0.556	0.209	0.552	0.206	0.551	0.206	0.551	0.206	0.551	0.2413

Table 27
Comparative Prioritization Results of The Criteria by The Various Molecular Geometry Shapes and Learning Rate.

Learning rate:0.1	Linear	Trigonal Planar	Tetrahedral	Trigonal Bipyramidal	Octahedral
CAEMEFF	3	3	3	3	3
RETINV	2	2	2	2	2
ENGCAPEX	1	1	1	1	1
ENVCOMSTD	4	4	4	4	4
Learning rate:0.5	**Linear**	**Trigonal Planar**	**Tetrahedral**	**Trigonal Bipyramidal**	**Octahedral**
CAEMEFF	3	3	3	3	3
RETINV	2	2	2	2	2
ENGCAPEX	1	1	1	1	1
ENVCOMSTD	4	4	4	4	4
Learning rate:1	**Linear**	**Trigonal Planar**	**Tetrahedral**	**Trigonal Bipyramidal**	**Octahedral**
CAEMEFF	3	3	3	3	3
RETINV	2	2	2	2	2
ENGCAPEX	1	1	1	1	1
ENVCOMSTD	4	4	4	4	4

Table 28
Averaged Fuzzy Numbers for Decision Matrix.

	CAEMEFF	RETINV	ENGCAPEX	ENVCOMSTD
SOLAR	(0.80, 0.15, 0.05)	(0.92, 0.07, 0.01)	(0.80, 0.15, 0.05)	(0.80, 0.15, 0.05)
WIND	(0.80, 0.15, 0.05)	(0.80, 0.15, 0.05)	(0.95, 0.05, 0.00)	(0.78, 0.16, 0.05)
GEOTHERMAL	(0.92, 0.07, 0.01)	(0.95, 0.05, 0.00)	(0.95, 0.05, 0.00)	(0.80, 0.15, 0.05)
BIOMASS	(0.95, 0.05, 0.00)	(0.95, 0.05, 0.00)	(0.80, 0.15, 0.05)	(0.95, 0.05, 0.00)
HYDROPOWER	(0.95, 0.05, 0.00)	(0.95, 0.05, 0.00)	(0.95, 0.05, 0.00)	(0.78, 0.16, 0.05)

Table 29
Weighted Decision Matrix.

	CAEMEFF	RETINV	ENGCAPEX	ENVCOMSTD
SOLAR	(0.20, 0.04, 0.01)	(0.24, 0.02, 0.00)	(0.21, 0.04, 0.01)	(0.19, 0.04, 0.01)
WIND	(0.20, 0.04, 0.01)	(0.20, 0.04, 0.01)	(0.24, 0.01, 0.00)	(0.19, 0.04, 0.01)
GEOTHERMAL	(0.23, 0.02, 0.00)	(0.24, 0.01, 0.00)	(0.24, 0.01, 0.00)	(0.19, 0.04, 0.01)
BIOMASS	(0.23, 0.01, 0.00)	(0.24, 0.01, 0.00)	(0.21, 0.04, 0.01)	(0.23, 0.01, 0.00)
HYDROPOWER	(0.23, 0.01, 0.00)	(0.24, 0.01, 0.00)	(0.24, 0.01, 0.00)	(0.19, 0.04, 0.01)

Table 30
Fuzzy Vectors for Decision Matrix.

Vectors	Fuzzy Vectors
y_1	[(0.20, 0.04, 0.01), (0.24, 0.02, 0.00), (0.21, 0.04, 0.01), (0.19, 0.04, 0.01)]
y_2	[(0.20, 0.04, 0.01), (0.20, 0.04, 0.01), (0.24, 0.01, 0.00), (0.19, 0.04, 0.01)]
y_3	[(0.23, 0.02, 0.00), (0.24, 0.01, 0.00), (0.24, 0.01, 0.00), (0.19, 0.04, 0.01)]
y_4	[(0.23, 0.01, 0.00), (0.24, 0.01, 0.00), (0.21, 0.04, 0.01), (0.23, 0.01, 0.00)]
y_5	[(0.23, 0.01, 0.00), (0.24, 0.01, 0.00), (0.24, 0.01, 0.00), (0.19, 0.04, 0.01)]

Table 31
Dot Products of Fuzzy Decision Vectors.

	$\boldsymbol{y}_1$	$\boldsymbol{y}_2$	$\boldsymbol{y}_3$	$\boldsymbol{y}_4$	$\boldsymbol{y}_5$
y_1		0.178	0.192	0.192	0.192
y_2	0.178		0.193	0.191	0.194
y_3	0.192	0.193		0.207	0.210
y_4	0.192	0.191	0.207		0.208
y_5	0.192	0.194	0.210	0.208	

Table 32
Cosine of Angle Between Fuzzy Decision Vectors.

	$\cos(\theta_{y_1})$	$\cos(\theta_{y_2})$	$\cos(\theta_{y_3})$	$\cos(\theta_{y_4})$	$\cos(\theta_{y_5})$
$\cos(\theta_{y_1})$		0.990	0.993	0.993	0.992
$\cos(\theta_{y_2})$	0.990		0.993	0.980	0.992
$\cos(\theta_{y_3})$	0.993	0.993		0.990	1.000
$\cos(\theta_{y_4})$	0.993	0.980	0.990		0.989
$\cos(\theta_{y_5})$	0.992	0.992	1.000	0.989	

Table 33
Angle In Radians for Decision Matrix.

	θ_{y_1}	θ_{y_2}	θ_{y_3}	θ_{y_4}	θ_{y_5}
θ_{y_1}		0.144	0.115	0.121	0.127
θ_{y_2}	0.144		0.117	0.202	0.126
θ_{y_3}	0.115	0.117		0.144	0.020
θ_{y_4}	0.121	0.202	0.144		0.150
θ_{y_5}	0.127	0.126	0.020	0.150	

Table 34
Normalized Angle Decision Values Using Different Molecular Geometry Shapes.

Linear	$norm(\theta_{y_1})$	$norm(\theta_{y_2})$	$norm(\theta_{y_3})$	$norm(\theta_{y_4})$	$norm(\theta_{y_5})$
$norm(\theta_{y_1})$	0.000	0.046	0.037	0.038	0.040
$norm(\theta_{y_2})$	0.046	0.000	0.037	0.064	0.040
$norm(\theta_{y_3})$	0.037	0.037	0.000	0.046	0.006
$norm(\theta_{y_4})$	0.038	0.064	0.046	0.000	0.048
$norm(\theta_{y_5})$	0.040	0.040	0.006	0.048	0.000
Trigonal Planar	$norm(\theta_{y_1})$	$norm(\theta_{y_2})$	$norm(\theta_{y_3})$	$norm(\theta_{y_4})$	$norm(\theta_{y_5})$
$norm(\theta_{y_1})$	0.000	0.069	0.055	0.058	0.061
$norm(\theta_{y_2})$	0.069	0.000	0.056	0.096	0.060
$norm(\theta_{y_3})$	0.055	0.056	0.000	0.069	0.010
$norm(\theta_{y_4})$	0.058	0.096	0.069	0.000	0.072
$norm(\theta_{y_5})$	0.061	0.060	0.010	0.072	0.000
Tetrahedral	$norm(\theta_{y_1})$	$norm(\theta_{y_2})$	$norm(\theta_{y_3})$	$norm(\theta_{y_4})$	$norm(\theta_{y_5})$
$norm(\theta_{y_1})$	0.000	0.076	0.060	0.063	0.066
$norm(\theta_{y_2})$	0.076	0.000	0.061	0.106	0.066
$norm(\theta_{y_3})$	0.060	0.061	0.000	0.075	0.011
$norm(\theta_{y_4})$	0.063	0.106	0.075	0.000	0.078
$norm(\theta_{y_5})$	0.066	0.066	0.011	0.078	0.000
Trigonal Bipyramidal	$norm(\theta_{y_1})$	$norm(\theta_{y_2})$	$norm(\theta_{y_3})$	$norm(\theta_{y_4})$	$norm(\theta_{y_5})$
$norm(\theta_{y_1})$	0.000	0.079	0.063	0.066	0.069
$norm(\theta_{y_2})$	0.079	0.000	0.064	0.110	0.069
$norm(\theta_{y_3})$	0.063	0.064	0.000	0.078	0.011
$norm(\theta_{y_4})$	0.066	0.110	0.078	0.000	0.082
$norm(\theta_{y_5})$	0.069	0.069	0.011	0.082	0.000
Octahedral	$norm(\theta_{y_1})$	$norm(\theta_{y_2})$	$norm(\theta_{y_3})$	$norm(\theta_{y_4})$	$norm(\theta_{y_5})$
$norm(\theta_{y_1})$	0.000	0.092	0.073	0.077	0.081
$norm(\theta_{y_2})$	0.092	0.000	0.075	0.128	0.080
$norm(\theta_{y_3})$	0.073	0.075	0.000	0.091	0.013
$norm(\theta_{y_4})$	0.077	0.128	0.091	0.000	0.095
$norm(\theta_{y_5})$	0.081	0.080	0.013	0.095	0.000

it is possible to develop renewable energy technologies. With these developing technologies, renewable energy production can be carried out much more cheaply. This situation also supports the development of the financial performance of the projects. In addition to them, for renewable energy projects to become more advantageous compared to fossil fuels, these projects must be able to produce electricity without interruption. To achieve this goal, the efficiency of energy storage processes must be increased. Energy production capacity can be expanded with a more successful storage system. This allows renewable energy projects to be uninterrupted. For projects to provide high return on investment, it is appropriate to implement certain policies. In this context, businesses should primarily take some actions that can reduce their costs. Investing in technologies and applications that will reduce energy consumption supports the achievement of this goal. In this way, it is possible to significantly reduce operational costs. On the other hand, developing

Table 35
Reciprocal Values of The Normalized Values.

	$\frac{1}{norm(\theta_{y_1})}$	$\frac{1}{norm(\theta_{y_2})}$	$\frac{1}{norm(\theta_{y_3})}$	$\frac{1}{norm(\theta_{y_4})}$	$\frac{1}{norm(\theta_{y_5})}$
$\frac{1}{norm(\theta_{y_1})}$		21.767	27.288	26.030	24.745
$\frac{1}{norm(\theta_{y_2})}$	21.767		26.800	15.591	24.880
$\frac{1}{norm(\theta_{y_3})}$	27.288	26.800		21.890	156.593
$\frac{1}{norm(\theta_{y_4})}$	26.030	15.591	21.890		20.966
$\frac{1}{norm(\theta_{y_5})}$	24.745	24.880	156.593	20.966	

Table 36
The Ranking Results.

	SOLAR	WIND	GEOTHERMAL	BIOMASS	HYDROPOWER	Aggregated values	Impact Directions
SOLAR		0.059	0.074	0.071	0.068	0.272	–
WIND	0.059		0.073	0.043	0.068	0.243	–
GEOTHERMAL	0.074	0.073		0.060	0.427	0.634	GEOTHERMAL → HYDROPOWER
BIOMASS	0.071	0.043	0.060		0.057	0.230	–
HYDROPOWER	0.068	0.068	0.427	0.057		0.620	HYDROPOWER → GEOTHERMAL

Table 37
Comparative Ranking Results of The Alternatives by The Different Molecular Geometry Shapes and Learning Rates.

Learning rate: 0.1	Linear	Trigonal Planar	Tetrahedral	Trigonal Bipyramidal	Octahedral
SOLAR	3	3	3	3	3
WIND	4	4	4	4	4
GEOTHERMAL	1	1	1	1	1
BIOMASS	5	5	5	5	5
HYDROPOWER	2	2	2	2	2
Learning rate: 0.5	**Linear**	**Trigonal Planar**	**Tetrahedral**	**Trigonal Bipyramidal**	**Octahedral**
SOLAR	3	3	3	3	3
WIND	5	5	5	5	5
GEOTHERMAL	1	1	1	1	1
BIOMASS	4	4	4	4	4
HYDROPOWER	2	2	2	2	2
Learning rate: 1	**Linear**	**Trigonal Planar**	**Tetrahedral**	**Trigonal Bipyramidal**	**Octahedral**
SOLAR	3	3	3	3	3
WIND	5	5	5	5	5
GEOTHERMAL	1	1	1	1	1
BIOMASS	4	4	4	4	4
HYDROPOWER	2	2	2	2	2

customer-focused strategies can also provide high return on investment. In this process, customer expectations should be analyzed in detail and understood. This situation allows the determination of strategies that can meet customer expectations more. Thanks to the developing customer satisfaction, the products of businesses can be preferred more. This situation also contributes significantly to the increase in the financial performance of projects.

Some practical application scenarios can be developed to demonstrate the impact of energy capacity expansion on environmental performance. In this context, production facilities can meet some of their daily energy needs by installing solar panels on factory roofs. The installation costs of these projects may be lower compared to other renewable energy alternatives. However, since they are small-scale projects, it is not possible for businesses to meet all of their energy needs in this way. Similarly, businesses can also take some actions to recycle waste energy. For example, waste heat obtained from machines operating at high temperatures can be used to heat the business. This allows businesses to significantly reduce their operational costs. Since this situation enables the long-term sustainability of projects, the environmental impacts of these investments increase positively. On the other hand, the use of smart grid technologies also contributes significantly to the development of this process. Smart grid systems support businesses to monitor their energy use in real time. This helps to optimize energy production processes.

CRediT authorship contribution statement

Hasan Dinçer: Writing – review & editing, Writing – original draft, Visualization, Validation, Supervision, Software, Resources, Project administration, Methodology, Investigation, Funding acquisition, Formal analysis, Data curation, Conceptualization. **Serhat Yüksel:** Writing – review & editing, Writing – original draft, Visualization, Validation, Supervision, Software, Resources, Project administration, Methodology, Investigation, Funding acquisition, Formal analysis, Data curation, Conceptualization. **Gabriela Oana Olaru:** Writing – review & editing, Writing – original draft, Visualization, Validation, Supervision, Software, Resources, Project administration, Methodology, Investigation, Funding acquisition, Formal analysis, Data curation, Conceptualization. **Serkan Eti:** Writing – review & editing, Writing – original draft, Visualization, Validation, Supervision, Software, Resources, Project administration, Methodology, Investigation, Funding acquisition, Formal analysis, Data curation, Conceptualization.

Declaration of competing interest

The authors declare that they have no known competing financial interests or personal relationships that could have appeared to influence the work reported in this paper.

Data availability

No data was used for the research described in the article.

References

[1] W. Zhang, B. Xi, The effect of carbon emission trading on enterprises' sustainable development performance: A quasi-natural experiment based on carbon emission trading pilot in China, Energy Policy 185 (2024) 113960.

[2] P.K.S. Rathore, B.S. Sikarwar, Thermal energy storage using phase change material for solar thermal technologies: A sustainable and efficient approach, *Sol. Energy Mater. Sol. Cells* 277 (2024) 113134.

[3] C. Quan, S. Feng, S. Gao, M. Zhang, C. Wu, N. Miskolczi, Sorption-enhanced ethanol steam reforming coupled with in-situ CO2 capture and conversion, *J. Energy Inst.* 101808 (2024).

[4] S. Orozco-Barrera, K. Wakabayashi, T. Yoshii, H. Nishihara, G.R. Iglesias, Á.V. Delgado, S. Ahualli, Polyelectrolyte-coated zeolite-templated carbon electrodes for capacitive deionization and energy generation by salinity exchange, *Separat. Purif. Technol.* (2024) 129314.

[5] Z. Zhao, M. Li, Y. Liu, X. Yu, T. Sang, P. Sun, Z. Li, Comparative study on combustion and emission of ternary-fuel combined supply SI engine with oxyhydrogen/ethanol/gasoline by different injection modes of fuel, *Case Stud. Therm. Eng.* 105015 (2024).

[6] M. Khishe, M. Mohammadi, A. Ramezani Varkani, Underwater backscatter recognition using deep fuzzy extreme convolutional neural network optimized via hunger games search, *Neural Process. Lett.* 55 (4) (2023) 4843–4870.

[7] K. Rahman, M. Khishe, Confidence level based complex polytopic fuzzy Einstein aggregation operators and their application to decision-making process, *Sci. Rep.* 14 (1) (2024) 15253.

[8] P.S. Kumar, Algorithms and software packages for solving transportation problems with intuitionistic fuzzy numbers, in: *Operational Research for Renewable Energy and Sustainable Environments*, IGI Global, 2024, pp. 1–55.

[9] C. Sugapriya, P. Saranyaa, D. Nagarajan, D. Pamucar, Triangular intuitionistic fuzzy number based backorder and lost sale in production, remanufacturing and inspection process, *Expert Syst. Appl.* 240 (2024) 122261.

[10] S.N. Abbasi, S. Ashraf, M. Akram, C. Jana, V. Simic, D. Pamucar, A Pythagorean fuzzy Z-number-based neutrality aggregation model for AI-enabled energy efficiency management, *Appl. Soft Comput.* 161 (2024) 111753.

[11] İ. Önden, M. Deveci, K. Kara, G.C. Yalçın, A. Önden, M. Eker, M. Hasseb, Supplier selection of companies providing micro mobility service under type-2 neutrosophic number based decision making model, *Expert Syst. Appl.* 245 (2024) 123033.

[12] A. Neumann, A. Hajji, M. Rekik, R. Pellerin, Genetic algorithms for planning and scheduling engineer-to-order production: a systematic review, *Int. J. Prod. Res.* 62 (8) (2024) 2888–2917.

[13] M. Kurucan, M. Özbaltan, Z. Yetgin, A. Alkaya, Applications of artificial neural network based battery management systems: a literature review, *Renew. Sustain. Energy Rev.* 192 (2024) 114262.

[14] F. Ecer, İ.Y. Ögel, H. Dinçer, S. Yüksel, Assessment of Metaverse wearable technologies for smart livestock farming through a neuro quantum spherical fuzzy decision-making model, *Expert Syst. Appl.* 255 (2024) 124722.

[15] G. Kou, D. Pamucar, S. Yüksel, H. Dinçer, M. Deveci, M. Umar, Evaluation of multidimensional carbon neutrality policies in transportation using a novel quantum picture fuzzy rough modelling, *IEEE Trans. Eng. Manag.* (2024).

[16] P.L. Gentili, The conformational contribution to molecular complexity and its implications for information processing in living beings and chemical artificial intelligence, *Biomimetics* 9 (2) (2024) 121.

[17] K. Deb, A. Pratap, S. Agarwal, T.A.M.T. Meyarivan, A fast and elitist multiobjective genetic algorithm: NSGA-II, IEEE Trans. Evol. Comput. 6 (2) (2002) 182–197.

[18] F. Xue, A. C. Sanderson, R. J. Graves, (2003, December). Pareto-based multi-objective differential evolution. In The 2003 Congress on Evolutionary Computation, 2003. CEC'03. (Vol. 2, pp. 862-869). IEEE.

[19] E. Zitzler, SPEA2: Improving the Strength Pareto Evolutionary Algorithm, 2001.

[20] D. Chauhan, R. Cheng, Competitive swarm optimizer: a decade survey, *Swarm Evol. Comput.* 87 (2024) 101543.

[21] R. Eberhart, Kennedy, J. (1995, November). Particle swarm optimization. In Proceedings of the IEEE international conference on neural networks (Vol. 4, pp. 1942-1948).

[22] V. Bulut, A. Onan, B. Senyayla, Obtaining the optimal shortest path between two points on a quasi-developable Bézier-type surface using the Geodesic-based Q-learning algorithm, *Eng. Appl. Artif. Intel.* 136 (2024) 108821.

[23] C. Ouyang, F. Yu, Y. Hao, Y. Tang, Y. Jiang, Build interval-valued time series forecasting model with interval cognitive map trained by principle of justifiable granularity, *Inf. Sci.* 652 (2024) 119756.

[24] B. Abhisheka, S.K. Biswas, B. Purkayastha, Infusing weighted average ensemble diversity for advanced breast cancer detection, *Int. J. Imaging Syst. Technol.* 34 (4) (2024) e23146.

[25] Q. Hassan, A.A. Khadom, S. Algburi, A.K. Al-Jiboory, A.Z. Sameen, M.A. Alkhafaji, M. Jaszczur, Implications of a smart grid-integrated renewable distributed generation capacity expansion strategy: The case of Iraq, *Renew. Energy* 221 (2024) 119753.

[26] L. Reichenberg, F. Hedenus, The error induced by using representative periods in capacity expansion models: system cost, total capacity mix and regional capacity mix, *Energy Syst.* 15 (1) (2024) 215–232.

[27] O. Usman, O. Ozkan, I. Adeshola, B.S. Eweade, Analysing the nexus between clean energy expansion, natural resource extraction, and load capacity factor in China: a step towards achieving COP27 targets. *Environment, Development and Sustainability*, 1-22.
[28] S. Papagianni, I. Capellán-Pérez, A. Adam, A. Pastor, Review and meta-analysis of Energy Return on Investment and environmental indicators of biofuels, *Renew. Sustain. Energy Rev.* 203 (2024) 114737.
[29] G. Suresh, Impact of financial literacy and behavioural biases on investment decision-making, *FIIB Business Review* 13 (1) (2024) 72–86.
[30] N. Scelles, Y. Inoue, S.J. Perkin, M. Valenti, Social impact assessment of corporate social responsibility initiatives: evaluating the social return on investment of an inclusion offer, *J. Bus. Ethics* (2024) 1–17.
[31] M. Ahmad, The role of recognition-based heuristics in investment management activities: are expert investors immune?–A systematic literature review, *Qualit. Res. Finan. Markets* 16 (3) (2024) 401–422.
[32] S. Yüksel, S. Eti, H. Dinçer, Y. Gökalp, D. Yavuz, A. Mikhaylov, G. Pinter, Prioritizing the indicators of energy performance management: A novel fuzzy decision-making approach for G7 service industries, *Environ. Res. Commun.* 6 (1) (2024) 015003.
[33] M.R. Seikh, P. Chatterjee, Determination of best renewable energy sources in India using SWARA-ARAS in confidence level based interval-valued Fermatean fuzzy environment, *Appl. Soft Comput.* 155 (2024) 111495.
[34] Y. Cheng, L. Jin, H. Fu, Y. Fan, R. Bai, Y. Wei, Investigating the impact of climate change and policy orientation on energy–carbon–water nexus under multi-criteria analysis, *Renew. Sustain. Energy Rev.* 189 (2024) 114032.
[35] F. Göçer, A novel extension of Fermatean fuzzy sets into group decision making: A study for prioritization of renewable energy technologies, *Arab. J. Sci. Eng.* 49 (3) (2024) 4209–4228.
[36] G. Şahin, A. Koç, W. van Sark, Multi-criteria decision making for solar power-Wind power plant site selection using a GIS-intuitionistic fuzzy-based approach with an application in the Netherlands, *Energ. Strat. Rev.* 51 (2024) 101307.
[37] Y. Zhou, X. Zhang, Y. Chen, X. Xu, M. Li, A water-land-energy-carbon nexus evaluation of agricultural sustainability under multiple uncertainties: The application of a multi-attribute group decision method determined by an interval-valued intuitionistic fuzzy set, *Expert Syst. Appl.* 242 (2024) 122833.
[38] İ. Otay, S.Ç. Onar, B. Öztayşi, C. Kahraman, Evaluation of sustainable energy systems in smart cities using a Multi-Expert Pythagorean fuzzy BWM & TOPSIS methodology, *Expert Syst. Appl.* 250 (2024) 123874.
[39] S. Naz, M. Akram, M.M. ul Hassan, A. Fatima, A hybrid DEMATEL-TOPSIS approach using 2-tuple linguistic q-rung orthopair fuzzy information and its application in renewable energy resource selection, *Int. J. Inf. Technol. Decis. Mak.* 23 (03) (2024) 1099–1142.
[40] M.H. Saeed, M. Saeed, A.U. Rahman, M. Ahsan, M.A. Mohammed, H.A. Marhoon, R. Martinek, Renewable energy resource management using an integrated robust decision making model under entropy and similarity measures of fuzzy hypersoft set, *Heliyon* 10 (13) (2024).